LONDON, METEOROLOGICAL OFFICE.

Met.O.19 Branch Memorandum No.74.

Statistifal retrieval of humidity profiles from TOVS data. By WATTS,P.D.

London,Met.Off.,Met.O.19 Branch Mem.No.74, 1984,31cm.Pp.21,24 pls.4 Refs.

An unofficial document - restriction on first page to be observed.

MET.0.19 BRANCH MEMORANDUM No. 74

STATISTICAL RETRIEVAL OF HUMIDITY PROFILES FROM TOVS DATA

by

P D WATTS

April 1984

Meteorological Office,
Met.0.19 (Satellite Meteorology branch),
London Road, Bracknell, Berks., RG12 2SZ

1. INTRODUCTION

The High-resolution Infra-red Radiation Sounder (HIRS-2) and Microwave Sounding Unit (MSU) on the TIROS-N series of polar-orbiting satellites provide global measurements from which temperature and humidity profiles may be retrieved. Humidity information is principally contained in data from 3 channels of HIRS-2 (channels 10, 11 and 12), although emission from water vapour makes a minor contribution to the radiances measured in some other channels. Temperature and humidity profiles are commonly retrieved by straightforward linear regression on the measured brightness temperatures. It will be shown that, while such a procedure is justified for temperature, the humidity problem is very non-linear and for best results should be treated as such. In this paper the linear regression of mixing ratio with brightness temperature is used as a control against which a new method of retrieval is tested. The latter involves the estimation of temperature using integrated water vapour as the vertical coordinate. The theory behind this approach is described in section 2.

Section 3 describes the origins of the data base used in the creation of the necessary statistics and explains how it is used to generate regression coefficients. The mechanics of extracting humidity information from the temperature profiles is explained in section 4, and the error analysis used to judge the relative effectiveness of a method in section 5. Finally, sections 6 and 7 present results and conclusions of the study.

2. THEORY

Temperature retrieval is commonly achieved by straightforward linear least squares regression on HIRS and MSU brightness temperatures. An analysis of the radiative transfer equation will show that this is theoretically justifiable :

$$R(\nu) = \int_{p_s}^{0} B(T(p),\nu).d\tau(p,0)/dp \,.\, dp + \tau(p_s,0)\{\varepsilon B(T_s,\nu) + (1-\varepsilon) R_{REF}(\nu)\} \quad \ldots\ldots 1.$$

where $R(\nu)$ is the radiance observed at the satellite at wavenumber ν,
$T(p)$ is the temperature of the atmosphere at pressure p,
$B(T,\nu)$ is the black-body function (source function of the radiation),
$\tau(p_1,p_2)$ is the transmission of the atmosphere from pressure p_1 to p_2,
ps and Ts are the surface pressure and temperature respectively,
ε is the surface emissivity (at ν)
and $R_{REF}(\nu)$ is the radiance emitted downwards by the atmosphere incident at the surface.

Therefore the first term on the right-hand side is the radiance from the atmosphere and is a weighted black-body function. The second term is the contribution from the surface and the third is the reflected component of downward atmospheric radiance. At infra-red wavelengths $\varepsilon \simeq 1$, and so for the purposes of this analysis the reflected term will be neglected.

Although equation 1 applies to monochromatic radiation, an expression of the same form can be used for a radiometer channel of finite bandwidth with the following provisos. $B(T(p),\nu)$ is replaced by an expression of similar form which is a weighted mean of the Planck function over the bandwidth of the channel. Similarly $\tau(p_1,p_2)$ is a mean transmittance over the bandwidth. Because the variation of B with temperature changes only slightly over the bandwidth of any channel, the errors introduced by this approximate formulation are small.

Equation 1 is exact in terms of Planck function profiles and radiances. More useful is an approximate form in terms of atmospheric temperature profiles and measured brightness temperatures respectively. With the approximation of $\varepsilon = 1$, we then obtain

$$t_B(\nu) = \int_{p_s}^{0} t(p)\, W(T,p)\, dp + t_s W_s \qquad \ldots\ldots\ldots 2.$$

where t(p) is the temperature profile expressed as a difference from a mean profile,

$t_B(\nu)$ is the brightness temperature expressed as a difference from a value appropriate to the mean profile,

$$W(T,p) = \frac{d\tau(p,o)}{dp} \cdot ff\left\{ \frac{dB(T(p),\nu)}{dT(p)}, \frac{dR(\nu)}{dT_B(\nu)} \right\}$$

and $$W_s = \tau(p_s,o) \cdot ff\left\{ \frac{dB(T_s,\nu)}{dT_s}, \frac{dR(\nu)}{dT_B(\nu)} \right\}$$

(Throughout this paper variables in lower case (excepting pressure, p) refer to differences from the mean.)

ff{} is found in practise to be only weakly temperature dependent. Also $\tau = e^{-\ell}$ where $\ell(p)$ is the optical depth of the atmosphere to pressure p from space, ie.,

$$\ell(p) = \int_{z(p)}^{\infty} k(z(p))\, \rho(z)\, dz \qquad \ldots\ldots\ldots 3.$$

k = absorption coefficient per unit density,
ρ = density (of absorber).

For a uniformly mixed gas such as carbon dioxide $\rho(z) = c\rho_{air}(z)$ where C is the constant mixing ratio. Therefore, because k is only weakly temperature dependent, ℓ is mainly a function of pressure. Consequently τ and therefore W $(= d\tau/dp)$ is sufficiently independent of temperature so as not to invalidate the linear theory given below. Because of the form of τ and the monotonic increase of ℓ with pressure, notice that

$W_s = \int_{\infty}^{p_s} W(p)\,dp$. So that we can rewrite the RHS of equation 2 :

$$\int_{p_s}^{0} t(p)\, W(p)\, dp + t_s W_s = \int_{p_s}^{0} t(p) W(p)\, dp + \int_{\infty}^{p_s} t_s W(p)\, dp = \int_{\infty}^{0} t(p)\, W(p)\, dp \qquad \ldots\ldots\ldots 4.$$

where for $P > P_s$, $t(p) = t_s$

the equation has thus been linearized and can be written in discrete form :

$$\underline{t_B} = \underline{\underline{W}} \cdot \underline{t(p)} \qquad \ldots\ldots\ldots 4a.$$

where vectors have components corresponding to the n channels and m

levels of profile discretization respectively. We wish to invert this using a predictive equation of the form

$$\underline{\hat{t}(p)} = \underline{\underline{D}} . \underline{t_B} \qquad \ldots\ldots\ldots 5.$$

(Variables with a circumflex refer to an estimated value rather than the true value.)

The predictive matrix $\underline{\underline{D}}$ can be found by numerous methods, linear least squares regression being simple and stable :

$$\underline{\underline{D}} = (\underline{t(p)} . \underline{t_B}) . (\underline{t_B} . \underline{t_B})^{-1} = \underline{\underline{S}}_{t(p),t_B} . \underline{\underline{S}}_{t_B,t_B} \qquad \ldots\ldots\ldots 6.$$

($\underline{\underline{S}}_{x,y}$ is the statistical covariance matrix of y with x.)

We could also attempt to retrieve humidity in the same way :

$$\underline{\hat{c}(p)} = \underline{\underline{D}}' . \underline{t_B}$$

but this implies $\underline{t_B} = \underline{\underline{k}}' . \underline{c(p)}$

or $$T_B(\nu) = \int c(p) . k'(p)\, dp$$

This is not a physically correct radiative tranfer equation because the temperature dependence of the radiance has been lost and because k' should be a function of c(p).

Following a method proposed (and tested) by Rosenkranz et al.(1976), we can implicity include water vapour into a temperature retrieval by using its integrated amount as an alternative vertical coordinate :

$$t_B(\nu) = \int_{u_s}^{0} t(u) W(u)\, du + t(u_s) W(u_s) \qquad \ldots\ldots\ldots 7.$$

where $u(p) = \int_p^0 c\, dp/g$, the overburden of water vapour at pressure p,

and $u_s = \int_{p_s}^0 c\, dp/g$, the surface overburden of water vapour.

Now, for a vertical path

$$\ell(u) = \int_0^{p(u)} k(p)\, c\, dp/g = ku \qquad \ldots\ldots\ldots 8.$$

where k is assumed almost constant (ie. neglecting the change of absorption coefficient due to pressure and temperature along the path of integration compared with that due to the change of mixing ratio). Therefore equation 7 is a valid temperature retrieval. Equation 8 is only a valid approximation for water vapour channels otherwise pressure is the dominating variable.

By analogy with equations 4 , 4a and 5 :

$$t_B(\nu) = \int_{\infty}^{0} t(u)\, W(u)\, du, \quad \text{where for } u > u_s \;\; t(u) = t(u_s) \qquad \ldots\ldots\ldots 9.$$

$$\underline{t_B} = \underline{\underline{K'(u)}} \cdot \underline{t(u)} \qquad \ldots\ldots\ldots 9a.$$

$$\underline{\hat{t}(u)} = \underline{\underline{D''}} \cdot \underline{t_B} \qquad \ldots\ldots\ldots 10.$$

By estimating temperature both as a function of pressure and of integrated water the vapour profile can be extracted as shown in figure 1. Shown is an ideal case in that both profiles are monotonically increasing and the temperature of the isothermal in $\hat{T}(U)$ (see section 3) is equal to $\hat{T}$(1000mb). Departures from this straightforward case are discussed in section 4. The retrieved humidity parameter in this instance is $\hat{U}(p)$ (integrated water amount). The control method produces $\hat{C}(p)$ (mixing ratio), integration of which is straightforward and accurate, random errors tending to cancel. Obtaining $\hat{C}(p)$ from $\hat{U}(p)$ by differentiation is less stable and a regression method is preferred. Appendix A gives the formulae for differentiating and integrating variables assuming linear and logarithmic dependencies.

The weighting functions of HIRS and MSU channels for a typical atmosphere are shown in figure 2. The water vapour channels are HIRS channels 10, 11 and 12, while other channels (principally 6, 7 and 8), though not designed to measure water vapour, are slightly sensitive to it. There can be seen to be reasonable coverage from 500mb to the surface and in principle, then, retrievals of water vapour mixing ratio should be possible in this region.

There is, however, a fundamental limitation on any method attempting to retrieve, from radiances, water vapour profiles in the near surface layers. Perturbation of the water vapour content at a level not only changes the radiance emitted from that level but also from all levels below by virtue of the change in transmittance of the path. If there is no temperature gradient below the perturbed layer, the increased water vapour will emit as much radiation as it absorbs from below. So that there will be zero sensitivity to absorber amount at a certain level if the atmosphere is isothermal below that level. Low temperature gradients will give a little information but the retrieval will be correspondingly sensitive to errors in the measured radiances and to those introduced in the inversion process. For this reason HIRS will tend to be relatively insensitive to low level water vapour, since there is usually little contrast between the temperature of these layers and the surface brightness temperature.

Eigenvector regression was used throughout this project because it has several distinct advantages over more traditional techniques (Smith and Woolf,1976). Most important of these is the method's insensitivity to assumed and actual noise levels - whether these are mismatched or not it produces near optimum results . Further, eigenvectors that are essentially only fitting noisy measurements can theoretically be identified by their eigenvalues and removed from the expansion. Thus truncated eigenvector regression coefficients are claimed to be insensitive to noise without oversmoothing retrievals.

Finally, all channels can be included in the regression despite the fact that most do not satisfy equations 9, 9a and 10. Such channels may supply some information but are substantially treated as noise and ignored. The fact that water vapour is correlated with temperature means that there is information on T(U) in carbon dioxide channels and their inclusion does improve the retrieval.

3. GENERATION OF REGRESSION COEFFICIENTS

For the purpose of testing the new algorithm it was decided to compare its resulting retrievals with those produced by straightforward regression of mixing raio against brightness temperature. Therefore it was reasonable to use synthetically derived radiances rather than collocated satellite/radiosonde pairs. This eliminates confusion due to inaccurate humidity and temperature measurements, and collocation errors. Two types of representative radiosonde data were available. Firstly the standard NESS set of 1200 profiles which was split into three latitude bands LOWLAT (from 0 to 30 deg.), MIDLAT (from 30 to 60 deg.) and HILAT (from 60 to 90 deg.) each of 400 profiles. Secondly, use was made of a set constructed for the European and N.Atlantic areas. This set contained 800 profiles for each month, 400 for land and 400 for coastal and oceanic based radiosonde stations, obtained from seven years of ascents (Pescod and Eyre, 1983). Data for September (SEPT) and June (JUN) was used in the study as well as a combined set of 40 profiles from each month (AMALG). All sets consisted of temperature and humidity data at non-standard pressure levels.

The synthetic radiances were obtained using TOVSRAD, a Met.O.19 program based on Madison's routines RAOBHIRS and RAOBMSU (Eyre, 1984). TOVSRAD interpolates the raw profile to 40 standard levels and calculates equivalent black body temperatures for 19 HIRS and 4 MSU channels, by numerical integration of the radiative transfer equation.

The general procedure for obtaining the coefficients is shown in figure 3. All statistical regressions are done using the routine CALCOF, which acts on covariance matrices of the predictors and predictands and includes an optional number of eigenvectors. Uncorrelated noise in the brightness temperatures is included into the regression by adding its expected variance along the diagonal elements of the covariance matrix. As suggested earlier, the effect of mismatched noise levels in eigenvector regression is supposed to be minimal but was tested nevertheless. The noise values used are obtained from studies of real data and are typical of the accuracies of cloud-cleared, limb-corrected brightness temperatures. In principle it is possible to find noise-fitting eigenvectors by their eigenvalues. In practice identification proved difficult and so the number of eigenvectors used was chosen empirically to minimise errors in a noisy independent data set. The exact number was not found to be critical and 9 eigenvectors were used in cases where there were 12 levels of discretization and 14 for the 24 U levels.

Three sets of so called 'primary' coefficients are calculated using program MAIN with profiles and brightness temperatures from the data set. These coefficients are all regressions on brightness temperatures : mixing ratio at fixed pressure levels, temperature at fixed pressure levels and temperature at fixed levels of integrated water vapour. For each profile T(p), C(p) and T are read from the data set and T(U) is calculated from T(p) and C(p). The first step is to integrate C(p) up to U(p) and this is done assuming logarithmic increase of C(p) for pressures lower than 700mb and a linear increase thereafter (see appendix A). Suitable interpolation of the U(p) profile with the T(p) profile gives T(U), the temperature at the 24 standard U levels.

As each profile is processed covariance matrices of t(p), c(p), $t_s(\nu)$ and t(U) are constructed. On completion these are submitted to CALCOF for calculation of the regression coefficients.

Two sets of 'secondary' coefficients are generated, 'secondary' in the sense that the predictor is itself a retrieved variable:

a) In order to test how much water vapour information can be extracted from the temperature profile alone, mixing ratio is regressed against retrieved temperature profile, the latter obtained using the 'primary' coefficients.
b) The new algorithm produces $\hat{U}(p)$ as the water vapour parameter. Retrieval of $\hat{C}(p)$ from $\hat{U}(p)$ by simple differentiation leads to large errors and substantial biases and a more stable route is to regress mixing ratio against the retrieved $\hat{U}(p)$ profiles. Regression takes account of the average gradient of $\hat{U}(p)$ about the pressure level concerned and consequently makes the resulting $\hat{C}(p)$ less sensitive to random errors in adjacent levels.

These 'secondary' coefficients are calculated by CALCOF. Data sets of retrieved $\hat{T}(p)$ and $\hat{U}(p)$ are generated by applying the 'primary' coefficients to the original brightness temperature set. Routine REG forms covariance matrices of these, and of c(p), and sends them to CALCOF for calculation of the coefficients.

Thus, in all, five sets of coefficients are calculated for each data-set.

4. APPLICATION OF RETRIEVAL METHOD

Once coefficients have been generated for a particular data set they can be used on any other set in a single program that simultaneously runs four methods of retrieving C(p) (see figure 4). To obtain the best from the new algorithm it is found necessary to 'tune' the various free parameters and to apply some empirical procedures to the peculiar problems associated with the interpolation routine, as explained below :

a) Standard U Levels

Since the quantity of water vapour varies considerably between data sets it is desirable to adjust the standard U levels so that the highest is equal to or just larger than the mean surface overburden. If the highest U level (U(24)) were made large enough to cover all sets then for some there would be a loss of resolution in T(U) as well as ill-defined isothermal regions (see below).

In accordance with mean profiles, U was made to vary logarithmically over its first 14 levels (from 0 mb to about 650 mb) and linearly thereafter. This also ensures an adequate number of levels in the more critical near-surface layers.

b) Non-Monotonic Profiles

Problems arise when interpolating between $\hat{T}(U)$ and $\hat{T}(p)$ levels when one or both of them are non-monotonic. Profiles with corresponding maxima and minima could be matched with sufficiently elaborate algorithms but this has not been done for two reasons. Firstly this is only a significant problem when there are many large scale inversions such as in Arctic regions (eg HILAT). Secondly it is in the nature of the radiative transfer equation for water that there is no information on mixing ratio when the atmosphere is isothermal from the surface (see section 2). It is doubtful, then, that retrievals from inverted or isothermal atmospheres would be of much value and so, in this study, retrievals involving non-monotonic temperature profiles were rejected.

c) Identification of Isothermal

As described in section 2, U levels greater than the surface overburden are assigned $\hat{T}$(1000mb) as their temperature. Therefore, an isothermal appearing in the retrieved $\hat{T}(U)$ vector indicates the surface overburden. However, depending on the spread of the U levels and the accuracy of the regression, the start of the isothermal will be more or less well defined. Figure 5 shows the tests made to confirm the existence of the surface isothermal; an increment in $\hat{T}(U)$ less than DT1 is the criterion for the start of an isothermal, DT2 checking that it is the surface isothermal and not a genuine atmospheric feature. The sizes of these two temperature increments are chosen empirically to minimise the bias on the retrieved $\hat{U}(p)$ vector.

d) Interpolation and Extrapolation

From the $\hat{T}(p)$ and $\hat{T}(U)$ profiles, $\hat{U}(p)$ is extracted by interpolating (logarithmically) as shown in figure 1.

Examination of individual retrievals shows that errors in $\hat{T}(U)$ and $\hat{T}(p)$ are not 100% correlated. They are correlated to some extent, as witnessed by the fact that $\hat{U}(p)$ derived from the true $T(p)$ vector is usually less accurate than that derived from the estimated vector $\hat{T}(p)$. Thus cases frequently occur where the $\hat{T}(p)$ vector terminates above the isothermal region in $\hat{T}(U)$, as shown in figure 6. At a first level of sophistication the identified isothermal is taken to indicate $\hat{U}(1000mb)$ and the assignment of near surface $\hat{U}(p)$ values undertaken as shown in the figure. When the $\hat{T}(p)$ vector terminates below the isothermal no problem arises.

For the case where no isothermal is present and the $\hat{T}(p)$ vector exceeds the $\hat{T}(U)$ vector, some sort of extrapolation is required. Figure 7 demonstrates the way in which half the $\hat{T}(U)$ profile is used for this, because extrapolations based on the last $\hat{T}(U)$ level interval are prone to be very unstable.

For cases where there is an isothermal in $\hat{T}(U)$ and the $\hat{T}(p)$ vector is displaced by a large amount (i.e. the profiles are inconsistent) it may be that one type of profile is more often in error. There are several possible ways of dealing these situations such as 'nudging' profiles together, ignoring isothermals, etc. Further study of this sort of discrepancy may lead to the identification of 'bad' retrievals and their subsequent discarding. Some of these refinements are discussed later.

5. METHOD OF ERROR ANALYSIS

As each profile is processed the estimated water parameters are compared to actual values and the error statistics are built up. Residual error (RE), variance (see appendix B) and mean vectors are calculated for $\hat{C}(p)$ and $\hat{U}(p)$ as well as the Fractional Unexplained Variance (FUV).

The RE squared may be described as the 'unexplained variance', that is, the variance in the data set not reproduced by the regression relation. This leads to FUV:

$$FUV = RE^2/VAR = 1/N \sum (y-\hat{y})^2 \Big/ 1/N \sum (y-\bar{y})^2$$

FUV is useful in two ways. Firstly it takes account of the variance of the data set so that comparisons between sets, or between subsections of a set, with different variances are possible. Secondly, with values ranging from 10^{-1} to 10^{3}, plotted REs are difficult to evaluate. All meaningful FUVs lie between 0 and 1 (between perfect and perfectly useless regression) and the relative success of different routes is more obvious.

6. RESULTS

6.1 RESULTS USING THE BASIC ALGORITHM

Henceforth the new algorithm will be denoted by UM (U method), the straightforward regression of C(p) versus t by PM and regression of C(p) versus retrieved T(p) by CT.

Initial tests done with independent and dependent data sets showed that there was little detrimental effect in using the former providing that it was from the same origin, for example, from the same month, if a monthly set was used to generate the coefficients. Since a valid comparison between the new and old algorithms is possible using dependant data, the set used to generate the coefficients is also used to carry out the error analysis (reducing the number of bulky files required). The sensitivity of the two methods to independent data though is of importance and results of a monthly set (SEPT), dependent and independent, are presented in figures 8 and 9. FUVs in the independent set are higher by about 0.04 at low levels and almost identical at pressures lower than 700mb. However, the relative performance of UM, PM and CT seem unaffected.

Table 1 gives the important characteristics of each of the data sets used, notably the generally high variances of MIDLAT and low variances of LOWLAT. Also note the freedom of most sets from significant numbers of inversions in the retrieved T(p) profiles. Figures 10 and 11 show the variances of T(U) and T(p) as a function of U level and pressure respectively. They serve to illustrate the high variance of MIDLAT (and to some extent HILAT) compared to other sets. The residual errors in predicting the temperature profiles are plotted in figure 12, and show that MIDLAT's errors are not as proportionately high as its variance.

Figures 13 to 16 show the FUVs in U(p) associated with the three methods, for LOWLAT, MIDLAT, HILAT and AMALG data (JUN results differed only marginally from SEPT and are not presented.) An overall conclusion that can be drawn is that there is a distinct gain (of between 0.1 and 0.2 units of FUV), generally, for pressures lower than 700mb with UM. Most sets show equal FUVs below this level down to 950mb or so and a bad performance by UM at 1000mb. U(1000) is of course the Total Precipitable Water content. The exception to this pattern is the MIDLAT set which shows distinct improvement right down to 950mb. This difference is due partly to a better UM performance and partly to a worse PM performance.

The MIDLAT data could be expected to favour UM because of its high water vapour variance which serves to exaggerate the non-linearity of PM. LOWLAT apparently has high variance U(p) (Table 1) but not if due regard is taken of its mean vapour content. With the set named AMALG (consisting of 480 profiles, 40 selected randomly from each of the 12 monthly sets, in an attempt to simulate the MIDLAT set) the mean vapour contents were comparable to MIDLAT, but variances are well down and the FUVs fell into the pattern of the other sets.

The CT method produced results that are reasonably easy to interpret. Generally CT improves (relative to other methods) towards the surface layers consistent with the loss of sensitivity of the radiances to water vapour in this region. This shows that PM and UM rely substantially on correlations with temperature at this level and so the performances of the three routes should be equal. However, both LOWLAT and AMALG depart from this rule in having large CT FUVs near the surface.

FUVs for mixing ratio with MIDLAT and SEPT are shown in figures 17 and 18 (the UM C(p) being the regressed version). They can be seen to be generally higher than FUV of $\hat{U}(p)$ values, this being expected for a derivative quantity. Figure 17 also shows the dew point errors associated with $\hat{C}(p)$ retrieval in MIDLAT derived from the mean temperature profile and RE of $\hat{C}(p)$.

6.2 FURTHER TREATMENT OF SURFACE PROBLEM

It was desirable at this stage to establish whether or not UM performance in low layers was being limited by a small group of 'bad' retrievals. In particular it would be interesting to see which types of retrieval, if any, were giving high 1000mb errors. Retrievals are thus split according to the type of interpolation required and separate error statistics compiled for each.

The five categories used were;

1. No Isothermal (in $\hat{T}(U)$)
2. False Isothermal — $\hat{T}(1000mb) >> \hat{T}(ISO)$, by >0.5K
3. True Isothermal — $\hat{T}(1000mb) > \hat{T}(ISO)$, but by <0.5K
4. Isothermal Irrelevent — $\hat{T}(1000mb) < \hat{T}(ISO)$, but by <1.5K
5. Isothermal Irr. large DT — $\hat{T}(1000mb) << \hat{T}(ISO)$, by >1.5K

The only change in interpolation procedure from that described in the previous sections was to ignore the isothermal in 2 and extrapolate.

Category 1 needed no change in interpolation procedure and generally produced results typical of the overall statistics, i.e. PM = UM below 700mb.

Category 2 was treated initially as,

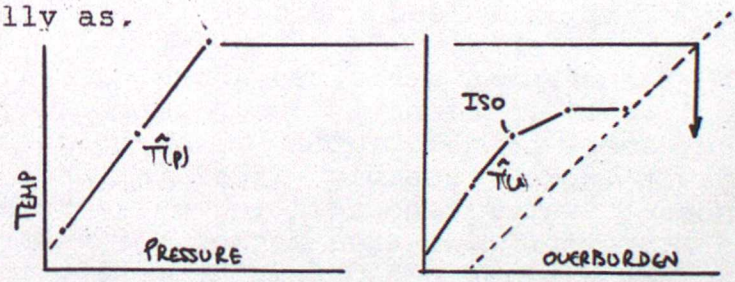

and the result was large surface biases. So the extrapolation was changed to,

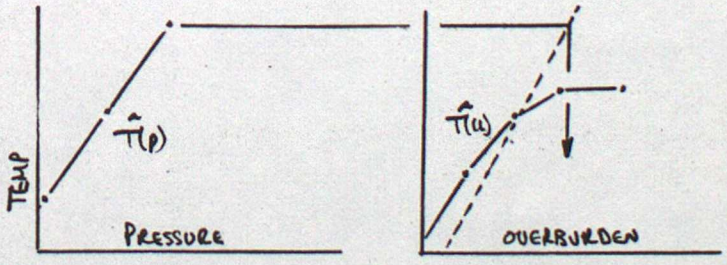

This improved the biases but this group still gave the worst UM-PM comparison.

Category 3 gave, initially, large surface biases which were removed by arbitrarily changing the U level to which U(1000mb) is tied. If level j was found to be the start of the isothermal then $\hat{U}(1000) = U(j-2)$. This is tantamount to changing the DTs in the isothermal detection but does not affect the other types of retrieval. 'True isothermals' do not do particularly well in UM.

Category 4 was a straightforward case with no end problems and

gave (at least with NESS sets) good results at pressures less than 950mb. Again the surface error was large, and this is evidence that this consistent feature is of more fundamental origin than simply incorrect treatment of the isothermal.

Category 5 gave much lower errors with UM even in the surface layers. As the constraint was tightened, i.e. the $\hat{T}(p)$ vector further divorced from the isothermal, results were better though numbers of retrievals in the category became minimal. Examination of individual retrievals revealed that they were almost invariably very low vapour/low temperature cases and thus reveal the inadequacies of PM (or superiority of UM) in dealing with extreme situations. PM, attempting to keep a linear relation between water vapour and brightness temperature, frequently produces negative mixing ratios in these cases.

Table 2 shows REs and FUVs for the five groups on SEPT and MIDLAT data.

A final check on whether some small number of 'bad' retrievals were present was a count of the frequency of r.e UM > r.e PM and vice versa, for the 850mb level where FUVs were generally equal ('r.e' indicates residual error on a single profile). Should these counts be approximately the same (i.e. about half the total) then the distribution of errors would be the same for both retrieval methods. It can be seen that, for the cases where the overall 850mb FUVs are similar, this is indeed the case (Table 3).

With the changes described above overall errors statistics were improved only marginally and this suggests that the near-surface problem cannot be alleviated by any improved interpolation scheme. The fault more probably lies in the insensitivity of infra-red radiances to water vapour in these layers and in the amplification of errors inherent in the method of extraction of $\mathbf{U}$. The largest improvement was for AMALG and the effect is shown on figure 16. At the other extreme, MIDLAT was barely affected.

6.3 NOISE LEVELS

Three runs were compared using SEPT and MIDLAT data to examine the effect of assumed and actual noise levels on the error statistics.

(A) Ordinary run : assumed noise (in regression) = actual noise (in forward run) = 0.4-0.8K (depending on channel).

(B) Low Noise run : as (A) with noise levels 0.1K in all channels

(C) Mismatched Noise : assumed noise = 0.1K , actual noise = 0.4-0.8K

Comparing the results of (B) and (C) with (A):

(B) Low noise levels had almost the same effect on both methods and between both sets of data (see figures 19 and 20) In the MIDLAT set the FUVs were down between .04 and .06 and for SEPT between .05 and .07. There were slight indications of a greater improvement in UM though probably not significant (eg. FUVs vary by ~ 0.02-0.04 as a consequence of changing the noise seed.)

(C) Susceptibility to mismatched noise was different between the sets (see figures 21 and 22). In MIDLAT, PM suffered only marginally losing about .01 FUV throughout. The effect on UM was erratic but between .06 and .10. In SEPT, PM suffered more, losing .08 to .03 from 1000mb to 300mb, while UM lost anything between .15 and .01, the latter figure around 780mb.

This exercise shows that UM is probably more susceptible to incorrect assumed noise despite eigenvector regression and despite correlation of retrieval errors in $\hat{T}(U)$ and $\hat{T}(p)$. From (B) it is clear that UM is not going to further improve its performance relative to PM with lower brightness temperature noise.

7. CONCLUSIONS

Rosenkranz et al in their initial test of the algorithm found very encouraging results with the UM algorithm. They made use of the 183 GHz water vapour channels (microwave) to estimate T(U) and 55 GHz oxygen band for T(p). The statistics they used were much more localised than any of the sets used in this study and consisted of far fewer soundings. Mean surface overburdens were about 58 Kg/m^2 and variances, though not quoted, were probably low considering the latitude and the number of soundings used. In terms of the results of this study they should not have done so well and the fact that they did probably reflects on the use of five microwave channels.

For water vapour sounding in the upper troposphere, the new algorithm, using HIRS channels, offers a significant increase in accuracy of retrieval. In the near surface layers the simpler and more stable approach appears to be PM although for soundings identified as being excessively 'dry' UM would be useful (UM does not gain at the 'wet' end due to the inaccuracies of extrapolation).

Further research with the algorithm as it stands could examine more categories of retrieval, as in the last section. For example, cases differentiated by degree of saturation, or types of temperature gradient present, may determine that it is advantageous to do the humidity retrieval one way or another. However the general impression gained from these studies is that there is a fundamental limitation on humidity retrieval using TOVS below 700mb and that any improvements will be minor and/or limited to a low percentage of retrievals. It was suggested earlier that the surface problem may well be due, at least in part, to a lack of information on water vapour in infra-red radiances. This information could be realised in the form of a good surface temperature estimate (e.g. from AVHRR (Advanced Very High Resolution Radiometer)) and a reasonably accurate Total Precipitable Water estimate (U(1000 mb)) from a 'Split Window'. Such estimates would be used to constrain the retrieved temperature profiles and would hopefully lead to more accurate retrievals.

The onset of microwave humidity sounders in the near future offers the best hope of substantial improvements in near surface water vapour retrieval (over the oceans at least). This is because the lack of contrast between surface brightness temperature and the low layer air temperature suffered by infra-red sounders is alleviated in the microwave region by surface emissivities significantly less than unity.

APPENDIX A
LINEAR AND LOGARITHMIC INTEGRATION AND DIFFERENTIATION

1. Linear $g\Delta u = \int_{p}^{p+\Delta p} \frac{1}{2}\left[c(p+\Delta p) + c(p)\right] dp$

$$= 1/2 \left[c(p+\Delta p) + c(p)\right] \Delta p \qquad \ldots\ldots\ldots A.1$$

2. Logarithmic

Assuming an exponential form of C(p): $C(p) = \alpha e^{\beta p}$

Then $\Delta u = \int_{p}^{p+\Delta p} \frac{\alpha e^{\beta p}}{g} dp = \frac{1}{g}\left[\frac{\alpha e^{\beta p}}{\beta} \right]_{p}^{p+\Delta p}$

$$= \frac{1}{g\beta}\left[c(p+\Delta p) - c(p)\right]$$

Now $c(p) = \alpha e^{\beta p}$ and $c(p+\Delta p) = \alpha e^{\beta(p+\Delta p)}$ so that $c(p+\Delta p)/c(p) = e^{\beta \Delta p}$

or $\beta = 1/\Delta p \, \mathrm{Log_e}\left[c(p+\Delta p)/c(p)\right]$

Therefore :

$$\Delta u = \left[c(p+\Delta p) - c(p)\right] \Big/ g \, \mathrm{Log_e}\left[c(p+\Delta p)/ c(p)\right] \qquad \ldots\ldots\ldots A.2$$

We have actually used the mean mixing ratio with respect to Log(p) i.e.;

$$\bar{c} = \mathrm{Exp}\left[1/2 \left\{ \mathrm{Log_e}(c(p+\Delta p)) + \mathrm{Log_e}(c(p))\right\}\right] = \sqrt{c(p+\Delta p).\, c(p)}$$

and $$\Delta u = \bar{c}\, \Delta p / g \qquad \ldots\ldots\ldots A.3$$

A.3 gives results differing only slightly from A.2. Considering the somewhat arbitary assignment of exponential form to C(p) this is acceptable.

Using the same assumptions, differentiating U(p) for C(p) gives,

Lin: $$C(p) = \frac{U(p+\Delta p) - U(p)}{\Delta p} . g = \frac{\Delta u\, g}{\Delta p} \qquad \ldots\ldots\ldots A.1a$$

Log: $$C(p) = \frac{U(p)\, g}{\Delta p} \mathrm{Log_e}\left[\frac{U(p+\Delta p)}{U(p)}\right] \qquad \ldots\ldots\ldots A.2a$$

or $$C(p+\Delta p) = \frac{\left(U(p+\Delta p) - U(p)\right)^2}{C(p)\, \Delta p^2} \qquad \ldots\ldots\ldots A.3a$$

APPENDIX B.

RESIDUAL ERRORS IN REGRESSION

If the predicted value of a variable y is $\hat{y}$ then the residual error is defined as:

$$e = y - \hat{y}$$

For many observations the mean of such residuals will tend to zero (identically zero for least squares regression) and so the rms value is used:

$$R_E^2 = \frac{1}{N}\sum (y-\hat{y})^2 \quad \text{..... (1)} \qquad N = \text{no. obs.}$$

$$= \frac{1}{N}\sum\left[(y-\bar{y}) - (\hat{y}-\bar{y})\right]^2$$

$$= \frac{1}{N}\sum\left[(y-\bar{y})^2 + (\hat{y}-\bar{y})^2 - 2(y-\bar{y})(\hat{y}-\bar{y})\right]$$

$$= \frac{1}{N}\left\{\sum (y-\bar{y})^2 + \sum (\hat{y}-\bar{y})^2 - 2\sum (\hat{y}-\bar{y})(y-\bar{y})\right\}$$

$$= \frac{1}{N}\left\{\quad " \quad + \quad " \quad - 2\sum (y-\bar{y})\,b(x-\bar{x})\right\}$$

$$= \frac{1}{N}\left\{\quad " \quad + \quad " \quad - 2b\sum (y-\bar{y})(x-\bar{x})\right\}$$

Since $(\hat{y}-\bar{y}) = b(x-\bar{x})$

If least squares regression is used, $b = \dfrac{\sum (y-\bar{y})(x-\bar{x})}{\sum (x-\bar{x})^2}$ ..... (2)

So that the 3rd term above becomes,

$$-2b^2\sum (x-\bar{x})^2$$
$$= -2\sum (\hat{y}-\bar{y})^2$$

or therefore :

$$R.E^2 = \frac{1}{N}\left\{\sum (y-\bar{y})^2 - \sum (\hat{y}-\bar{y})^2\right\} \quad \text{..... (3)}$$

Combining (1) and (3) :

$$\sum (y-\bar{y})^2 = \sum (y-\hat{y})^2 + \sum (\hat{y}-\bar{y})^2$$

Sum of squares of actual about mean = S. Sq. of actual about regression + S. Sq of regression about mean

That is, the variance of actual values about the mean can be 'explained' by the variance of actual values about predicted values, and that of predicted values about the mean.

For an accurate regression equation $\sum (y-\hat{y})^2$ is small.

Alternative formula for sum of squares:

Of regression about mean: $\sum (\hat{y}-\bar{y})^2 = b\{\sum xy - (\sum x)(\sum y)/N\}$

Of actual about mean: $\sum (y-\bar{y})^2 = \sum y^2 - (\sum y)^2/N$

Of actual about regression $\sum (y-\hat{y})^2$ by subtraction

If the regression relation is multivariate, i.e. $y = b + b_1x_1 + \ldots\ldots b_\Lambda x_\Lambda$ an analysis of variance can show which of the x_i are important in explaning y and therefore which are worth retaining in the regression relation.

Multivariate Regression

If we have Λ_y predictants, $y_1, y_2 \ldots\ldots y_{\Lambda y}$ and Λ_x predictors, $x_1, x_2 \ldots x_{\Lambda x}$ where $y_i = y_i - \bar{y}_i$ etc, then the regression relation is best expressed as,

$$y = Cx, \quad \ldots\ldots\ldots\ldots \textcircled{4}$$

$$(\Lambda_y \times k) = (\Lambda_y \times \Lambda_x)(\Lambda_x \times k)$$

y, e, x being matrices of the dimensions shown, k is the number of observations.

The result of least squares regression is that $C = yx^T(xx^T)^{-1}$ ..... ⑤

And the residual errors are now given by,

$$R.\mathcal{E}^2 = \frac{1}{N}(y-\hat{y})(y-\hat{y})^T$$

since diagonal elements of the resulting matrix are $\frac{1}{N}\sum (y_i-\hat{y}_i)^2$.

Off diagonal elements give information on the correlation between residuals in different variables;

$$R.\mathcal{E}^2_{ij} = \frac{1}{N}\sum (y_i-\hat{y}_i)(y_j-\hat{y}_j)$$

So the residual error matrix is;

$$R.\mathcal{E}^2 = \frac{1}{N}(y-\hat{y})(y^T-\hat{y}^T)$$

$$= \frac{1}{N}\{yy^T - \hat{y}y^T - y\hat{y}^T + \hat{y}\hat{y}^T\}$$

And substituting $\hat{y} = Cx$:

$$R.\varepsilon^2 = \frac{1}{N}\left\{ yy^T - Cxy^T - y(Cx)^T + Cx(Cx)^T \right\}$$

$$= \frac{1}{N}\left\{ yy^T - Cxy^T - yx^TC^T + Cxx^TC^T \right\} \quad \text{..... (6)}$$

$$\left[(AB)^T = B^TA^T \right]$$

Taking the second term of (6);

$$Cxy^T = yx^T(xx^T)^{-1}xy^T$$

$$= yx^T\left(yx^T\left((xx^T)^{-1} \right)^T \right)^T$$

and being symmetric, $(xx^T)^{-1} = ((xx^T)^{-1})^T$.

$$\therefore \quad \underline{Cxy^T} = yx^T\left(yx^T(xx^T)^{-1}\right)^T = \underline{yx^TC^T}$$

So that (6) becomes;

$$\underline{R.\varepsilon^2 = \frac{1}{N}\left\{ yy^T - 2yx^TC^T + Cxx^TC^T \right\}}$$

The last term $Cxx^TC^T = yx^T.(xx^T)^{-1}xx^T.C^T$

$$= yx^T \cdot \underline{\underline{1}} \cdot C^T = yx^TC^T$$

Therefore, finally:

$$\underline{\underline{R.\varepsilon^2 = \frac{1}{N}\left\{ yy^T - yx^TC^T \right\}}} \quad \text{..... (7)}$$

Eigenvector treatment of the regression equation gives,

$$C = yx^Tx^*\left[x^{*T}(xx^T)x^* \right]^{-1}x^{*T}$$

where x^* is a matrix of some or all of the eigenvectors of matrix x (the matrix of predictors).

Substitution of this C matrix into (6) gives again equation (7) for the residual error matrix.

In analogy to analysis of variance above, an analysis of the eigenvalues gives the relative importance of corresponding eigenvectors in the regression relation.

REFERENCES

(1) P.W.Rosenkranz, M.J.Komichak and D.H.Staelin, (1982). 'A Method for Estimation of Atmospheric Water Vapour Profiles by Microwave Radiometry'. J.Appl.Meteor., 21, 1364-1370

(2) W.L.Smith and H.M.Woolf, (1976). 'The Use of Eigenvectors of Statistical Covariance Matrices for Interpreting Satallite Sounding Radiometer Observations'. J.Atmos.Sci, 33(7), 1127-1140.

(3) R.W.Pescod and J.R.Eyre, (1983). 'Accumulation of a Set of Radiosonde Profiles For Use With Satallite Sounding Data From the European and North Atlantic Areas'. MET O 19 Branch Memorandum No.71.

(4) J.R.Eyre, (1984). 'TOVSRAD User Guide', Met.O.19 Working paper (in preparation)

TABLE 1. DATA-SET CHARACTERISTICS

	LOWLAT	MIDLAT	HILAT	SEPT	JUN	AMALG
$\overline{U(1000\,mb)}$	33.0	14.9	9.5	18.5	18.4	14.5
$\sigma\, U(1000\,mb)$	10.5	10.1	5.9	7.5	–	7.3
$\overline{C(1000\,mb)}$	13.9	5.6	2.4	7.6	7.6	5.8
$\sigma^2 T(u)$	19	160	169	55	–	150
$\sigma^2 T(p)$	19	188	198	45	–	62
No. of Non-Monotonic $\hat{T}(p)$	0	66	120	0	–	1

$\overline{U(1000\,mb)}$ – Mean surface overburden (Kg/M^2)

$\sigma\, U(1000\,mb)$ – Standard deviation of surface overburden (kg/M^2)

$\overline{C(1000\,mb)}$ – Mean surface mixing ratio (g/Kg)

$\sigma^2 T(u)$ – Variance of T(U) (for $U_i = 24$) (K^2)

$\sigma^2 T(p)$ – Variance of T(p) (for p = 1000mb) (K^2)

TABLE 2. CATEGORIZED ERROR STATISTICS ON U(p)

A) SEPTEMBER DATA

CATEGORY 1 (No Isothermal) no. profiles = 116

P(mb):	RE/U:	RE/P:	VAR:	FUV/U:	FUV/P:	BIAS/U:
100	0.018	0.004	0.00	99.900	99.900	0.006
200	0.021	0.022	0.00	1.095	1.224	-0.013
300	0.041	0.054	0.00	0.418	0.743	-0.004
400	0.120	0.169	0.05	0.278	0.554	-0.003
500	0.321	0.402	0.38	0.270	0.422	-0.025
620	0.665	0.784	1.94	0.228	0.317	-0.047
700	1.086	1.132	4.17	0.283	0.308	0.126
780	1.748	1.739	8.42	0.363	0.359	-0.038
850	2.457	2.398	14.15	0.426	0.406	-0.747
920	3.303	3.105	21.53	0.507	0.448	-1.358
950	3.451	3.401	25.17	0.473	0.460	-0.714
1000	4.596	3.891	32.47	0.650	0.466	0.186

RE = residual error
VAR = variance (U(p))
FUV = fractional unexplained var
BIAS = bias of $\hat{U}(p)$ from true U(p)
/U = UM
/P = PM

CATEGORY 2 (False Isothermal) no. profiles = 198

P(mb):	RE/U:	RE/P:	VAR:	FUV/U:	FUV/P:	BIAS/U:
100	0.028	0.005	0.00	99.900	99.900	0.015
200	0.025	0.021	0.00	1.752	1.218	-0.016
300	0.036	0.039	0.00	0.515	0.614	-0.011
400	0.085	0.103	0.03	0.248	0.371	-0.010
500	0.186	0.222	0.20	0.171	0.245	-0.043
620	0.406	0.449	1.06	0.156	0.190	-0.037
700	0.784	0.798	2.76	0.223	0.231	0.109
780	1.436	1.384	6.10	0.338	0.314	0.173
850	2.132	2.038	10.34	0.440	0.402	-0.068
920	2.785	2.699	16.28	0.476	0.447	-0.386
950	3.160	2.981	20.03	0.499	0.444	-0.034
1000	4.320	3.484	28.75	0.649	0.422	-0.060

CATEGORY 3 (True Isothermal) no. profiles = 23

P(mb):	RE/U:	RE/P:	VAR:	FUV/U:	FUV/P:	BIAS/U:
100	0.057	0.006	0.00	99.900	99.900	0.030
200	0.045	0.017	0.00	8.888	1.226	-0.004
300	0.053	0.034	0.00	1.647	0.660	-0.030
400	0.057	0.070	0.01	0.280	0.428	0.004
500	0.125	0.221	0.08	0.201	0.629	-0.008
620	0.201	0.449	0.34	0.120	0.601	-0.010
700	0.432	0.653	0.76	0.244	0.559	0.046
780	0.773	0.908	1.96	0.305	0.420	-0.198
850	1.473	1.452	4.77	0.454	0.441	-0.738
920	2.621	2.214	10.65	0.645	0.460	-1.302
950	2.930	2.517	14.58	0.589	0.435	-1.117
1000	4.541	3.004	23.68	0.871	0.381	-1.691

CATEGORY 4 (Isothermal Irrelevant) no. profiles = 54

P(mb):	RE/U:	RE/P:	VAR:	FUV/U:	FUV/P:	BIAS/U:
100	0.050	0.005	0.00	99.900	99.900	0.029
200	0.046	0.022	0.00	6.893	1.579	0.000
300	0.063	0.040	0.00	2.856	1.154	-0.042
400	0.075	0.098	0.01	0.550	0.950	-0.012
500	0.110	0.195	0.04	0.284	0.886	-0.006
620	0.169	0.385	0.19	0.153	0.790	0.028
700	0.426	0.638	0.53	0.342	0.769	0.048
780	0.810	0.880	1.10	0.597	0.705	0.044
850	1.124	1.141	2.25	0.561	0.578	-0.087
920	1.800	1.584	5.41	0.599	0.463	-0.284
950	2.161	1.829	8.07	0.579	0.415	-0.065
1000	3.830	2.333	15.06	0.974	0.361	1.507

CATEGORY 5 (Isothermal Irrelevant: large T(1000)-T(ISO))
no. profiles = 6

P(mb):	RE/U:	RE/P:	VAR:	FUV/U:	FUV/P:	BIAS/U:
100	0.073	0.003	0.00	99.900	99.900	0.042
200	0.049	0.005	0.00	106.155	1.226	0.013
300	0.035	0.010	0.00	6.231	0.520	-0.030
400	0.052	0.042	0.00	2.076	1.328	0.042
500	0.100	0.149	0.01	0.888	1.997	0.081
620	0.162	0.463	0.09	0.308	2.517	0.114
700	0.155	0.877	0.24	0.101	3.237	0.029
780	0.423	1.491	0.57	0.312	3.876	-0.347
850	0.849	2.067	1.18	0.609	3.609	-0.762
920	0.882	2.676	1.92	0.405	3.723	-0.705
950	0.729	2.976	2.15	0.247	4.122	-0.450
1000	0.943	3.582	2.44	0.364	5.252	0.702

B) MIDLAT DATA

CATEGORY 1 (No Isothermal) no. profiles = 151

P(mb):	RE/U:	RE/P:	VAR:	FUV/U:	FUV/P:	BIAS/U:
100	0.004	0.001	0.00	99.900	99.900	0.001
200	0.008	0.008	0.00	1.162	1.242	-0.003
300	0.026	0.030	0.00	0.428	0.592	-0.002
400	0.066	0.145	0.05	0.086	0.417	-0.002
500	0.196	0.382	0.54	0.071	0.270	0.024
620	0.516	0.880	3.34	0.080	0.232	-0.077
700	1.060	1.483	8.49	0.132	0.259	-0.085
780	1.662	2.160	17.63	0.157	0.265	-0.403
850	2.311	2.751	29.87	0.179	0.253	-0.518
920	3.002	3.550	48.97	0.184	0.257	-0.480
950	3.827	3.975	60.16	0.243	0.263	-0.061
1000	6.240	4.883	84.98	0.458	0.281	1.008

CATEGORY 2 (False Isothermal) no. profiles = 49

P(mb):	RE/U:	RE/P:	VAR:	FUV/U:	FUV/P:	BIAS/U:
100	0.002	0.001	0.00	99.900	99.900	0.001
200	0.004	0.005	0.00	0.719	1.211	-0.002
300	0.018	0.019	0.00	0.518	0.631	-0.004
400	0.045	0.069	0.01	0.165	0.387	-0.009
500	0.154	0.177	0.13	0.183	0.243	-0.041
620	0.272	0.287	0.73	0.101	0.113	-0.135
700	0.555	0.648	2.03	0.152	0.207	0.124
780	1.183	1.298	5.18	0.270	0.325	0.295
850	2.204	2.088	10.84	0.448	0.402	0.799
920	3.330	3.040	20.59	0.539	0.449	0.597
950	4.229	3.478	26.27	0.681	0.461	0.658
1000	5.955	4.297	38.48	0.922	0.480	0.361

CATEGORY 3 (True Isothermal) no. profiles = 29

P(mb):	RE/U:	RE/P:	VAR:	FUV/U:	FUV/P:	BIAS/U:
100	0.004	0.001	0.00	99.900	99.900	0.001
200	0.006	0.007	0.00	0.926	1.144	-0.002
300	0.025	0.026	0.00	0.732	0.781	-0.009
400	0.053	0.083	0.01	0.234	0.568	-0.025
500	0.108	0.183	0.07	0.169	0.489	-0.015
620	0.214	0.350	0.28	0.163	0.436	0.008
700	0.537	0.543	0.77	0.374	0.382	0.187
780	0.791	0.947	1.77	0.353	0.507	0.195
850	1.630	1.581	3.55	0.748	0.703	0.640
920	2.167	2.415	7.77	0.605	0.751	0.619
950	2.737	2.806	10.94	0.684	0.719	0.834
1000	4.245	3.565	19.29	0.934	0.659	0.753

CATEGORY 4 (Isothermal Irrelevant) no. profiles = 80

P(mb):	RE/U:	RE/P:	VAR:	FUV/U:	FUV/P:	BIAS/U:
100	0.005	0.001	0.00	99.900	99.900	0.002
200	0.004	0.004	0.00	1.424	1.231	-0.001
300	0.015	0.016	0.00	1.356	1.524	-0.005
400	0.031	0.069	0.00	0.432	2.159	-0.001
500	0.083	0.222	0.03	0.214	1.530	-0.005
620	0.161	0.518	0.25	0.104	1.076	-0.061
700	0.423	0.840	0.89	0.201	0.793	-0.004
780	0.785	1.293	2.47	0.250	0.678	-0.055
850	1.274	1.828	5.10	0.318	0.656	0.104
920	2.060	2.497	9.71	0.437	0.642	-0.129
950	2.561	2.803	12.59	0.521	0.624	-0.107
1000	4.054	3.362	19.25	0.853	0.587	0.837

CATEGORY 5 (Isothermal Irrelevant: large T(1000)-T(ISO))
no. profiles = 25

P(mb):	RE/U:	RE/P:	VAR:	FUV/U:	FUV/P:	BIAS/U:
100	0.004	0.001	0.00	99.900	99.900	0.001
200	0.003	0.003	0.00	1.973	2.085	-0.001
300	0.011	0.017	0.00	1.269	3.176	-0.005
400	0.018	0.089	0.00	0.313	7.603	-0.004
500	0.040	0.266	0.02	0.097	4.174	-0.001
620	0.101	0.631	0.13	0.078	3.075	-0.033
700	0.219	1.022	0.40	0.120	2.607	0.016
780	0.447	1.590	1.15	0.174	2.203	-0.217
850	0.863	2.309	2.80	0.266	1.902	-0.491
920	1.853	3.164	5.91	0.581	1.694	-1.216
950	2.330	3.542	7.69	0.706	1.630	-1.496
1000	3.205	4.209	11.45	0.897	1.548	-1.855

TABLE 3. 850 MB ERROR COMPARISON

	FUV $\hat{u}(p)$			No. OF ERRORS	
	P_M	U_M		$\epsilon_{PM} > \epsilon_{UM}$	$\epsilon_{UM} > \epsilon_{PM}$
LOWLAT	.144	.157		199	202
MIDLAT	.208	.136		205	130
HILAT	.225	.227		157	122
SEPT	.191	.204		194	204
AMALG	.194	.180		293	187

No. $\epsilon_{PM} > \epsilon_{UM}$ indicates the frequency with which an individual retrieval error obtained with PM was greater than that obtained with UM.

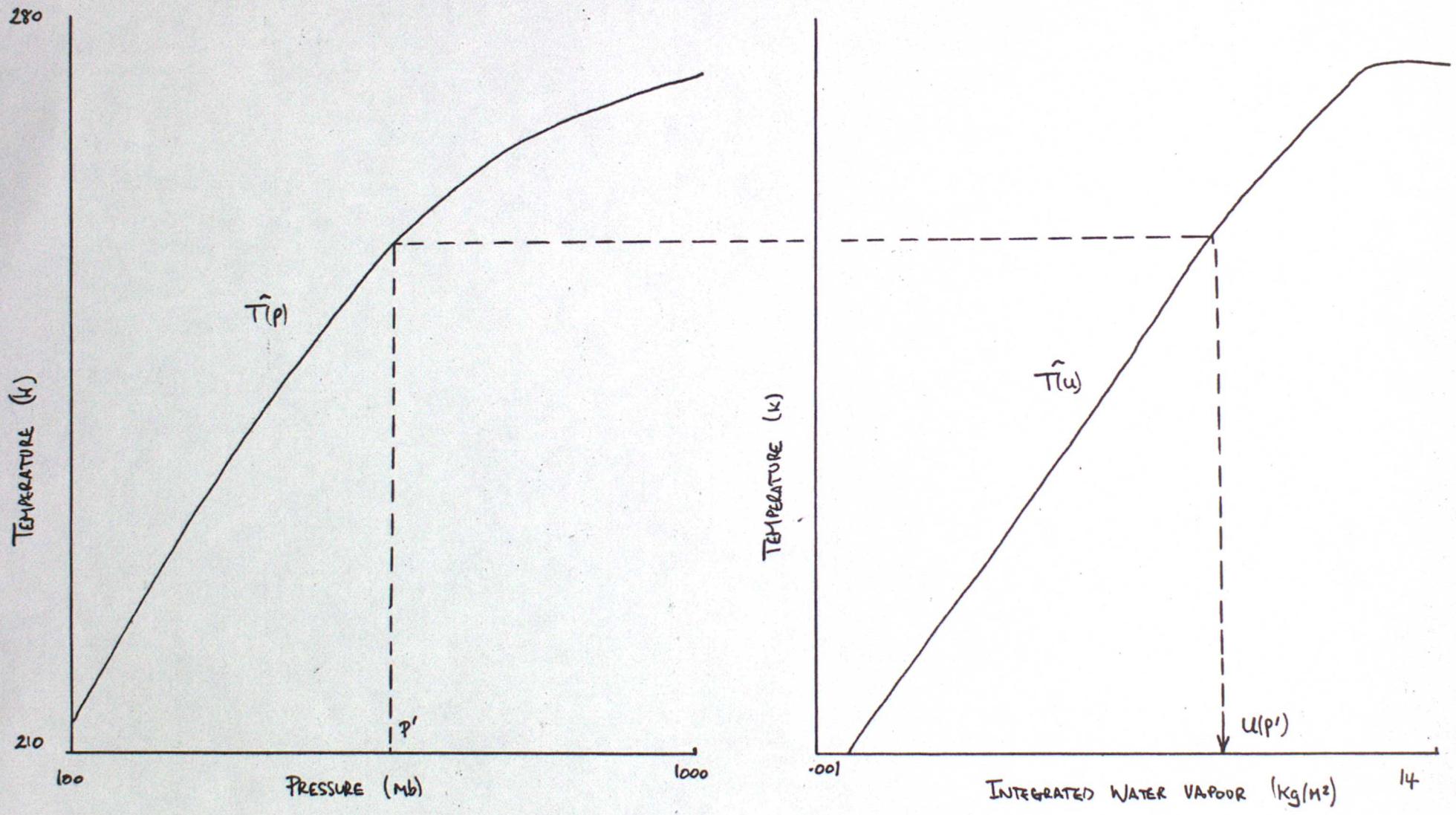

Fig 1. INTERPOLATION OF $\hat{T}(u)$ & $\hat{T}(p)$ PROFILES FOR $\hat{u}(p)$

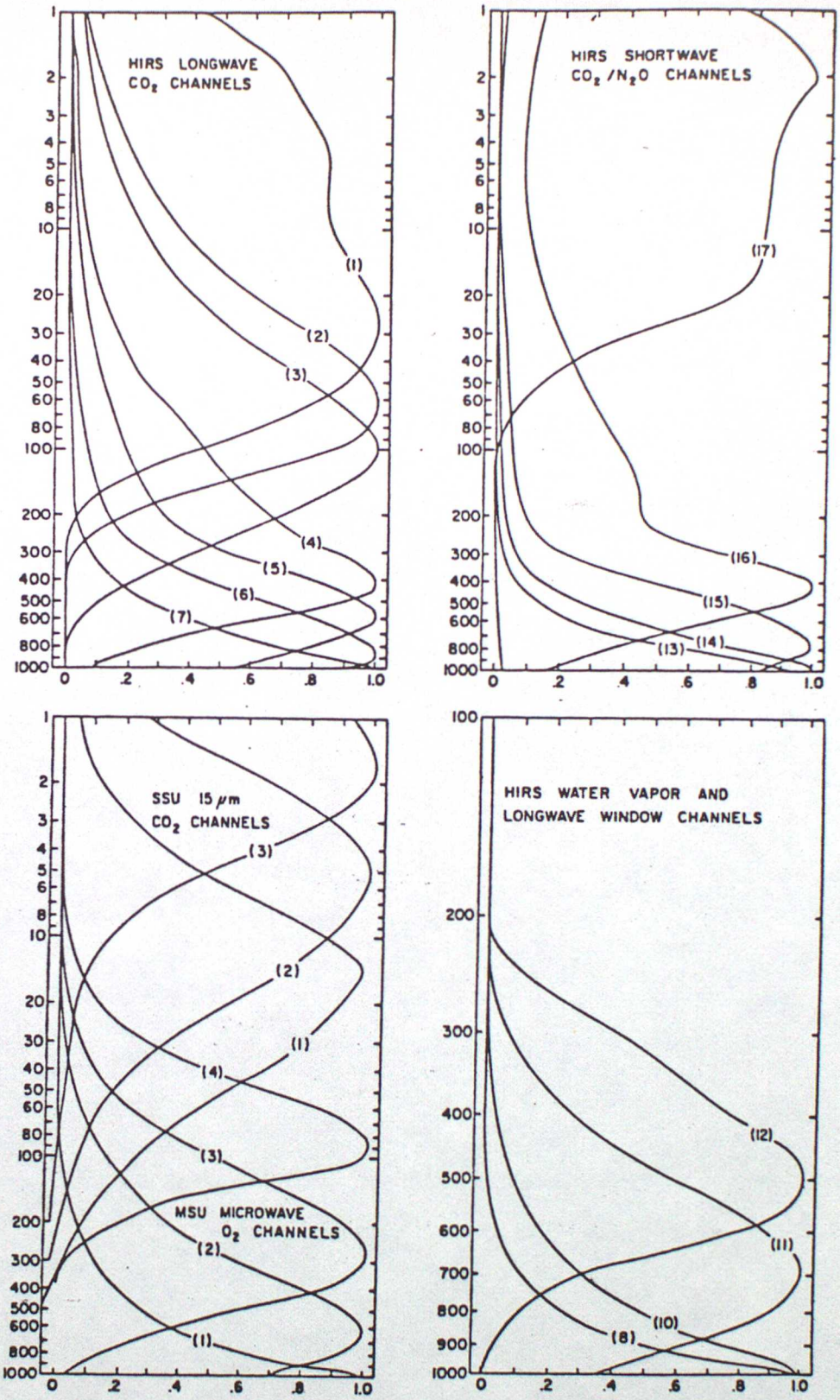

TOVS weighting functions (normalized).

Fig. 2.

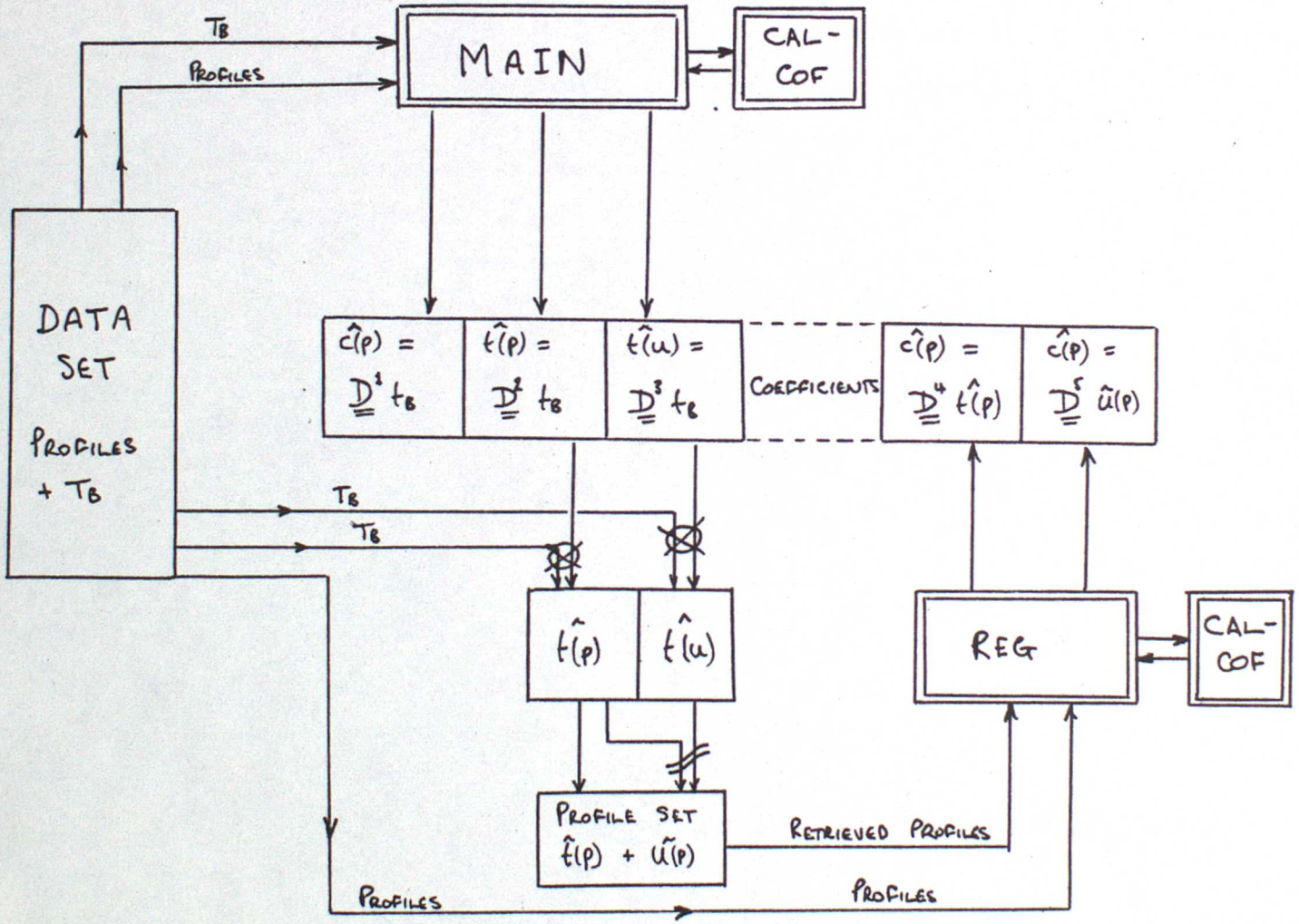

FIG 3. COEFFICIENT GENERATION

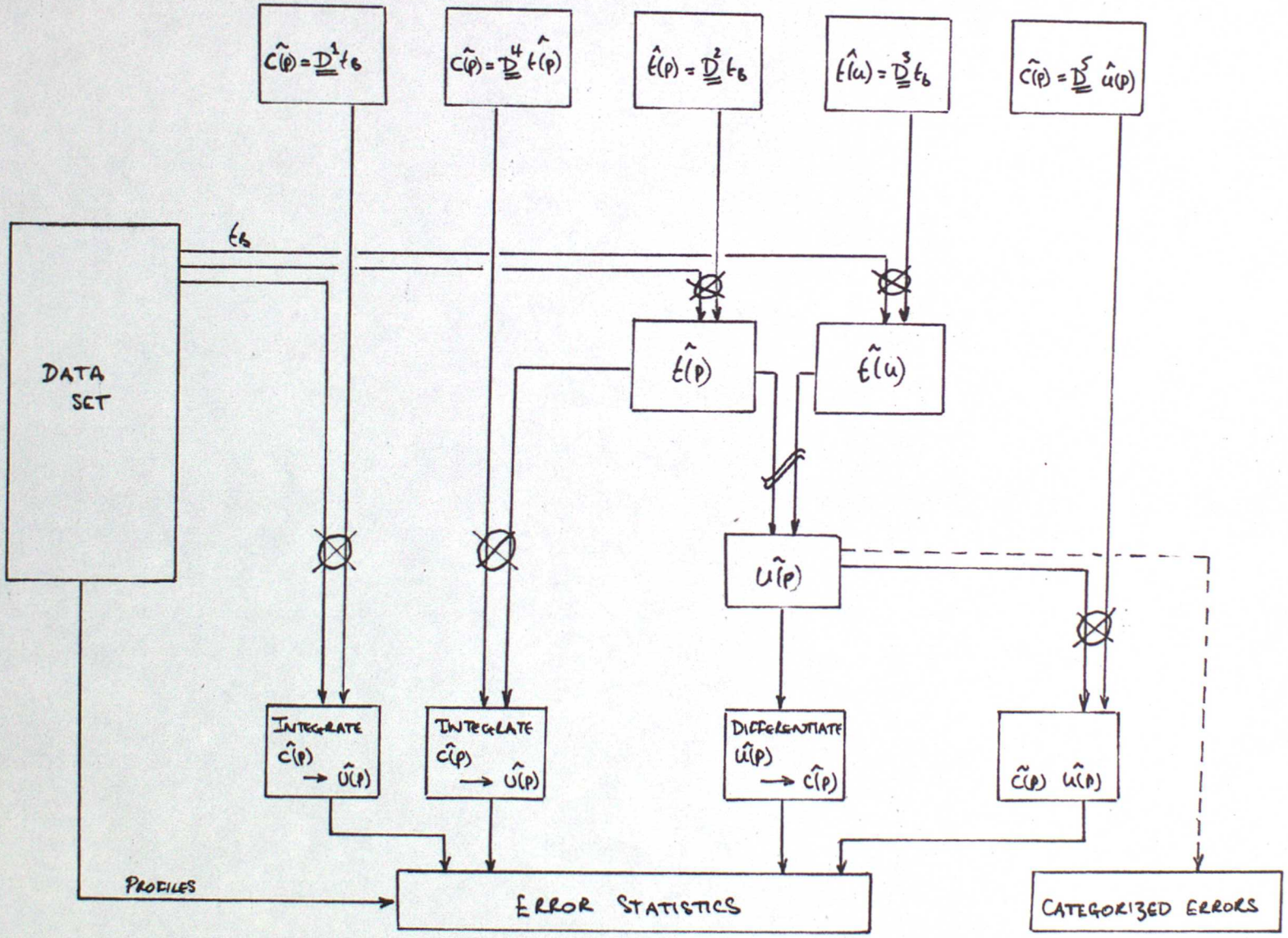

FIG 4. ERROR ANALYSIS

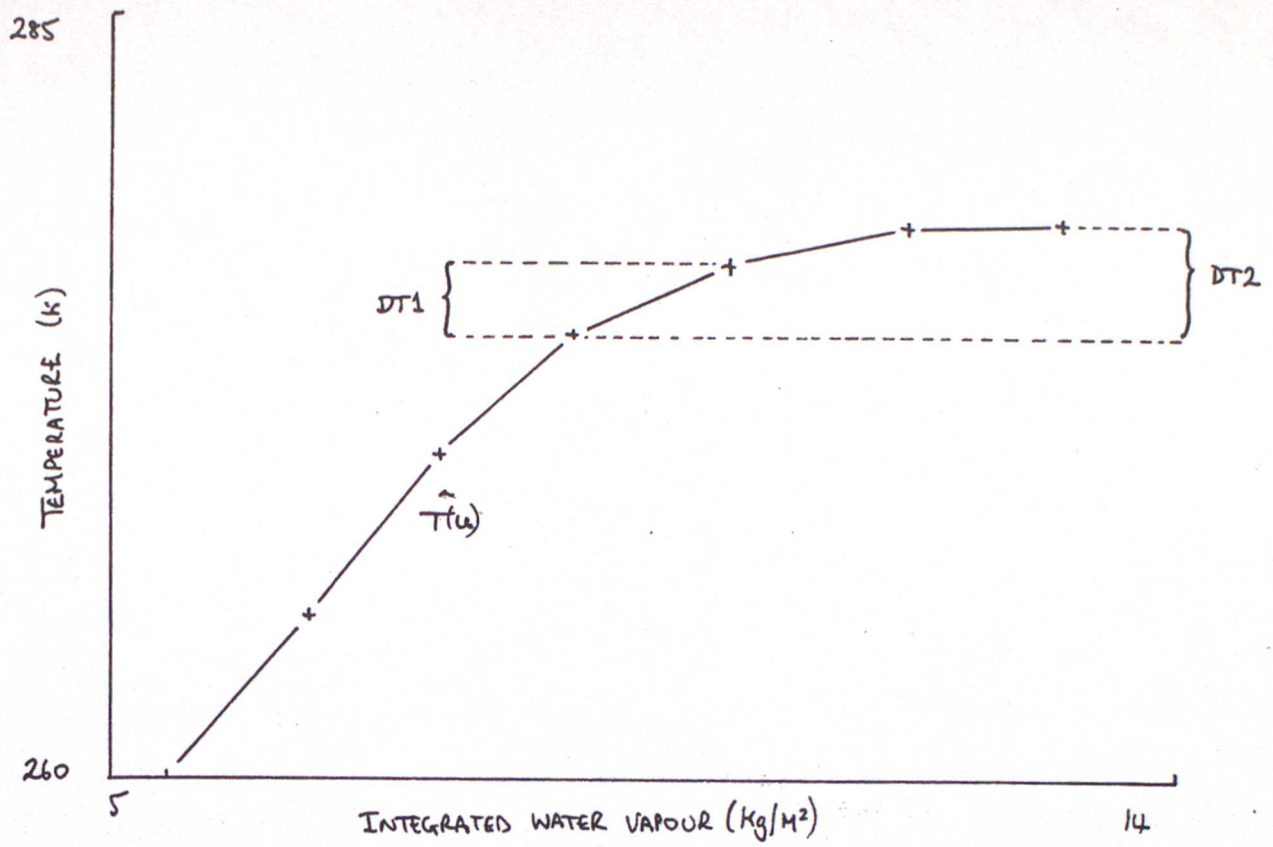

Fig 5. DETERMINATION OF ISOTHERMAL

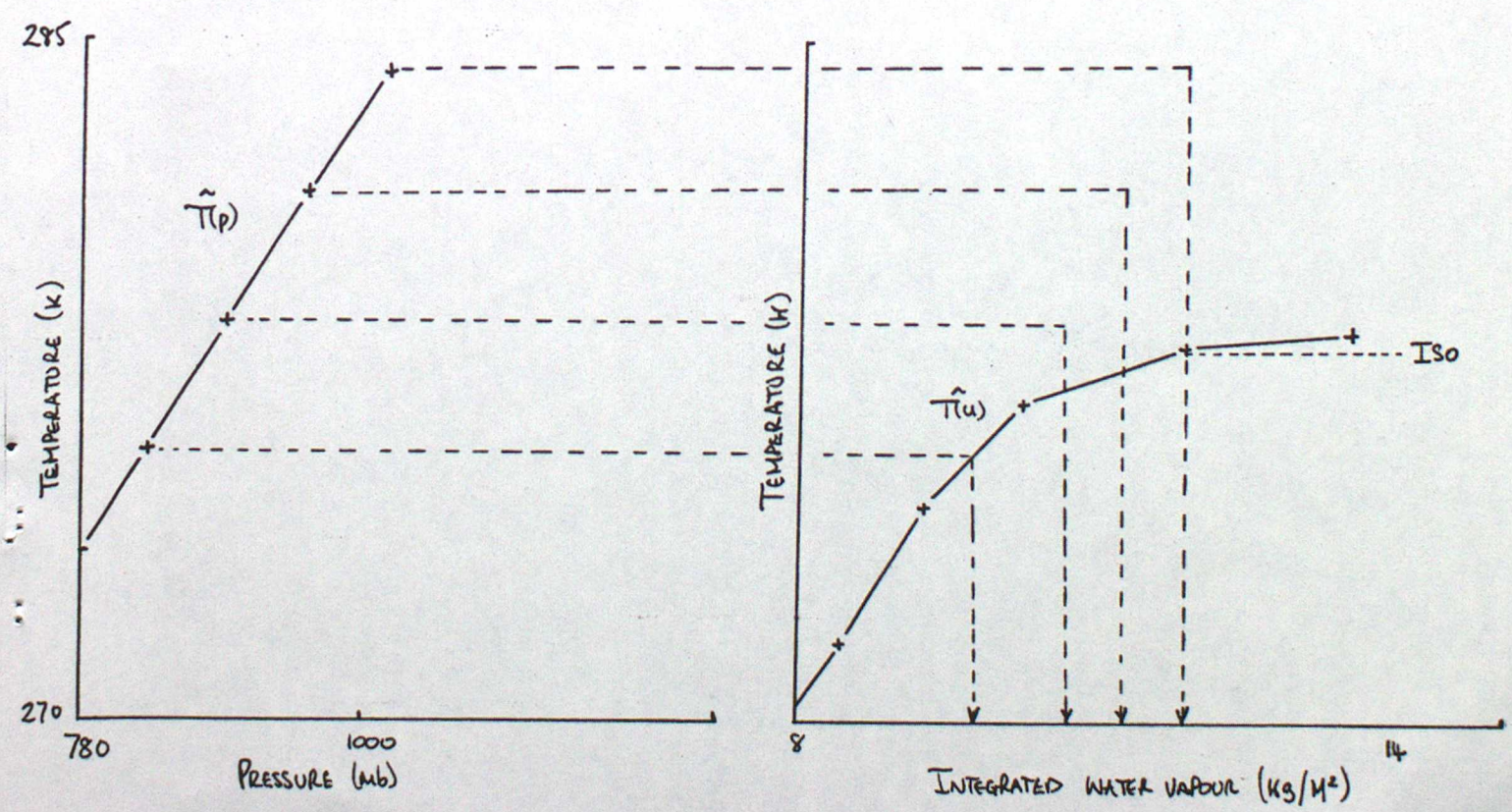

Fig 6. DISPLACED $\tilde{T}(p)$ and $\hat{T}(u)$ PROFILES

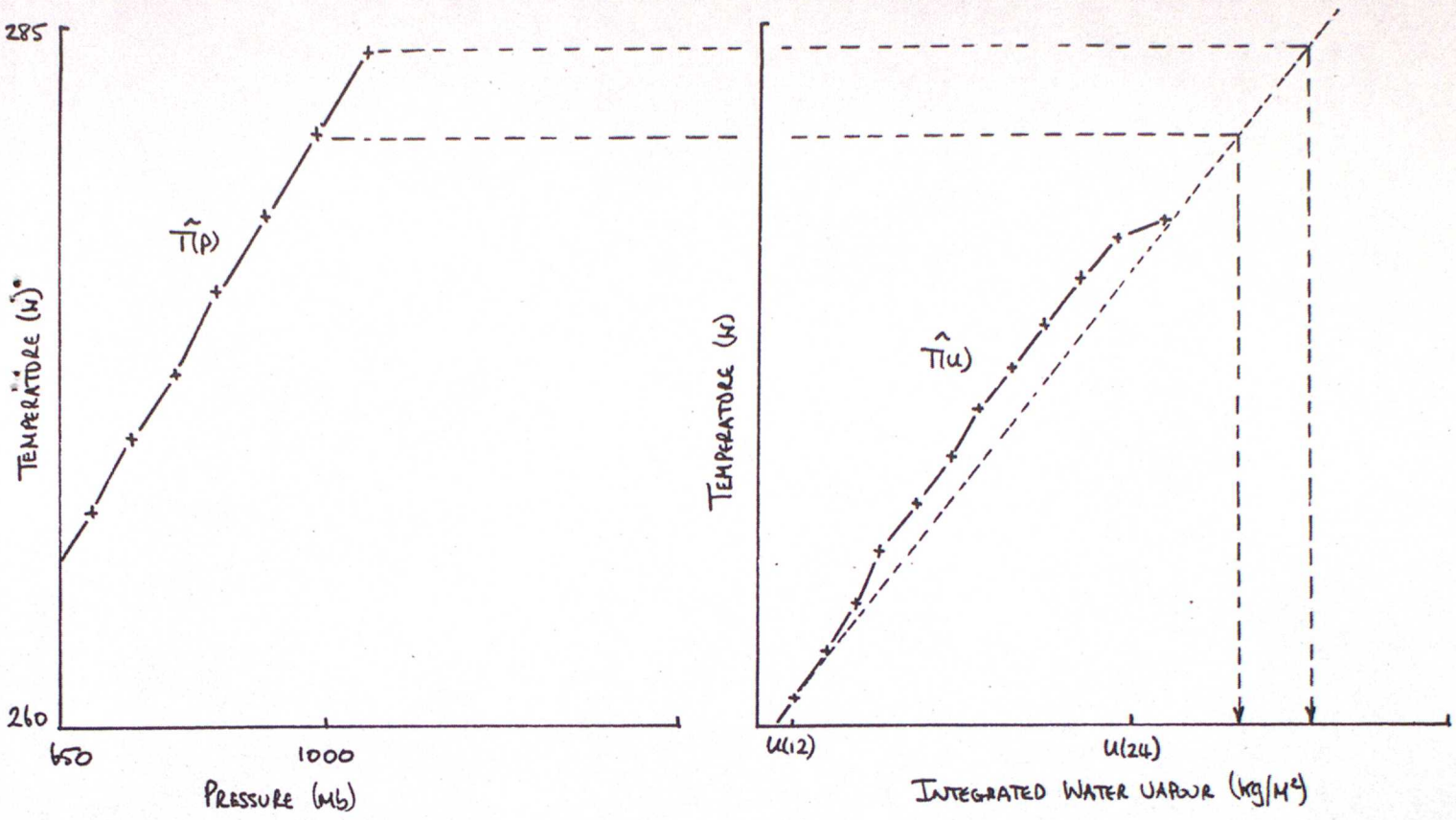

Fig 7. EXTRAPOLATION ON 1/2 PROFILE

Figure 8

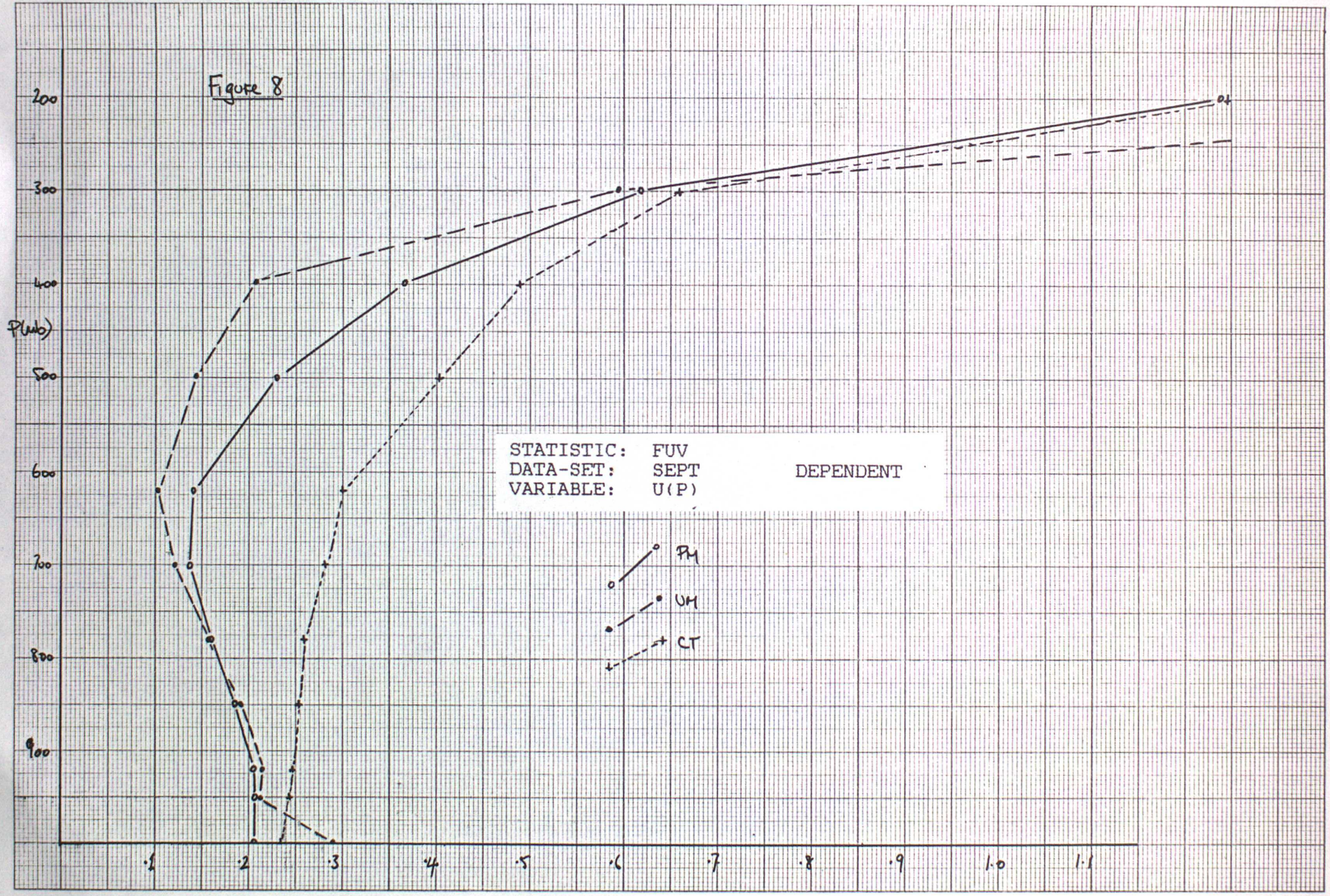
200
300
400
P(mb)
500
600
700
800
900
.1
.2
.3
.4
.5
.6
.7
.8
.9
1.0
1.1
STATISTIC: FUV
DATA-SET: SEPT
VARIABLE: U(P)
DEPENDENT
PM
UM
CT

Figure 9

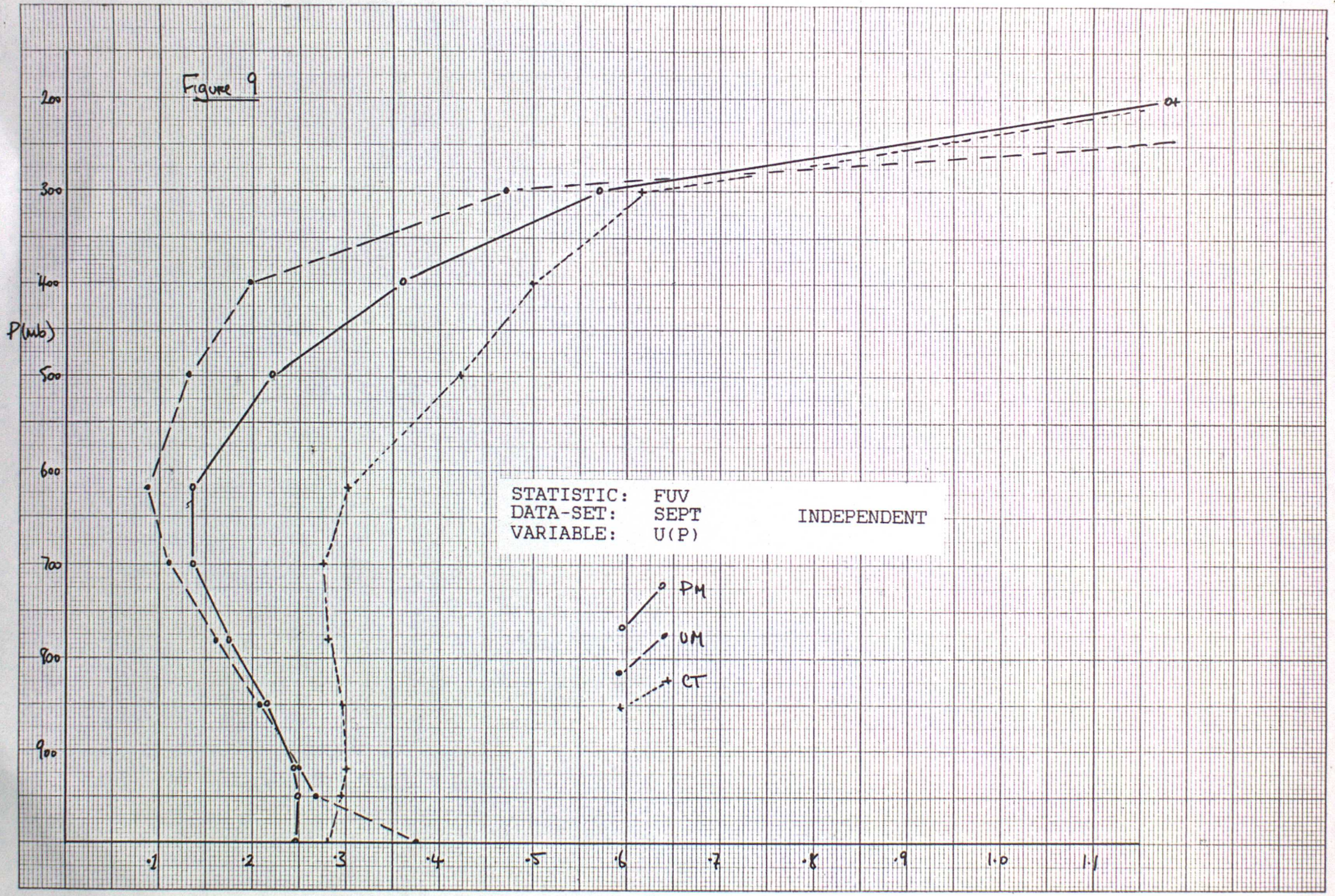
200
300
400
P(mb)
500
600
700
800
900
.1
.2
.3
.4
.5
.6
.7
.8
.9
1.0
1.1
STATISTIC: FUV
DATA-SET: SEPT
VARIABLE: U(P)
INDEPENDENT
PM
UM
CT

Figure 10

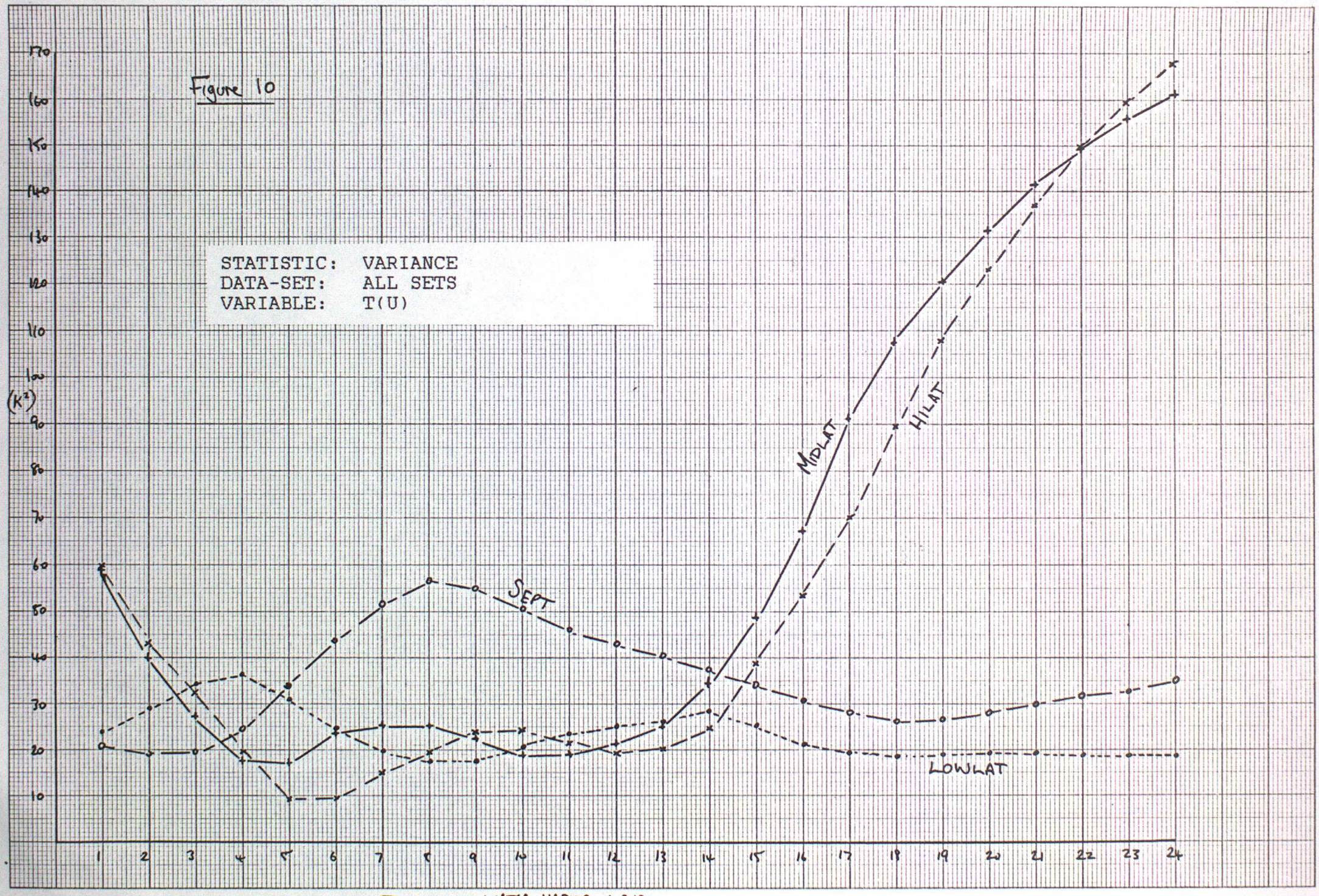
STATISTIC: VARIANCE
DATA-SET: ALL SETS
VARIABLE: T(U)
(K²)
170
160
150
140
130
120
110
100
90
80
70
60
50
40
30
20
10
SEPT
MIDLAT
HILAT
LOWLAT
1 2 3 4 5 6 7 8 9 10 11 12 13 14 15 16 17 18 19 20 21 22 23 24
INTEGRATED WATER VAPOUR LEVEL

Figure 11

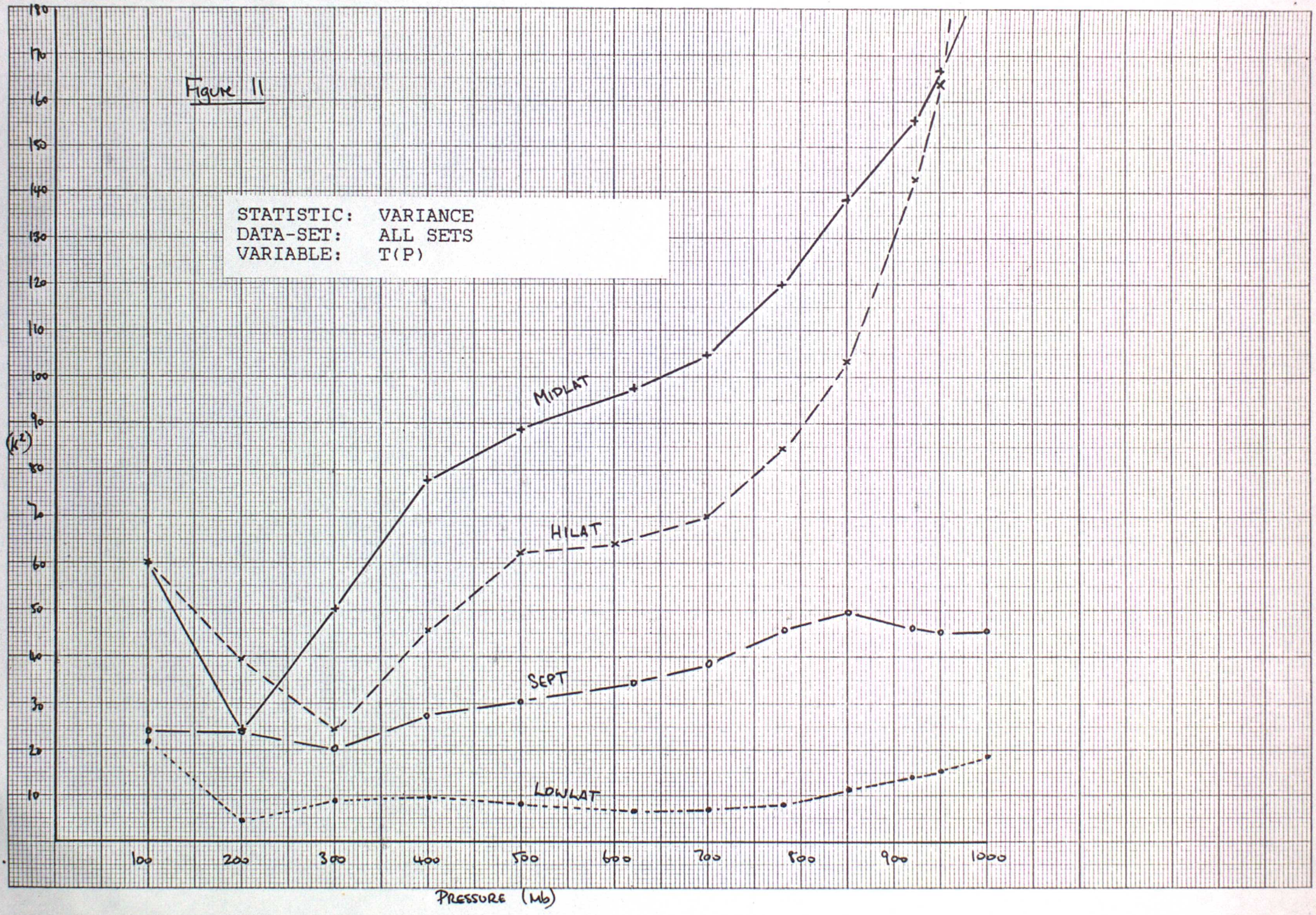
STATISTIC: VARIANCE
DATA-SET: ALL SETS
VARIABLE: T(P)
MIDLAT
HILAT
SEPT
LOWLAT
(K²)
PRESSURE (MB)
100
200
300
400
500
600
700
800
900
1000

Figure 12

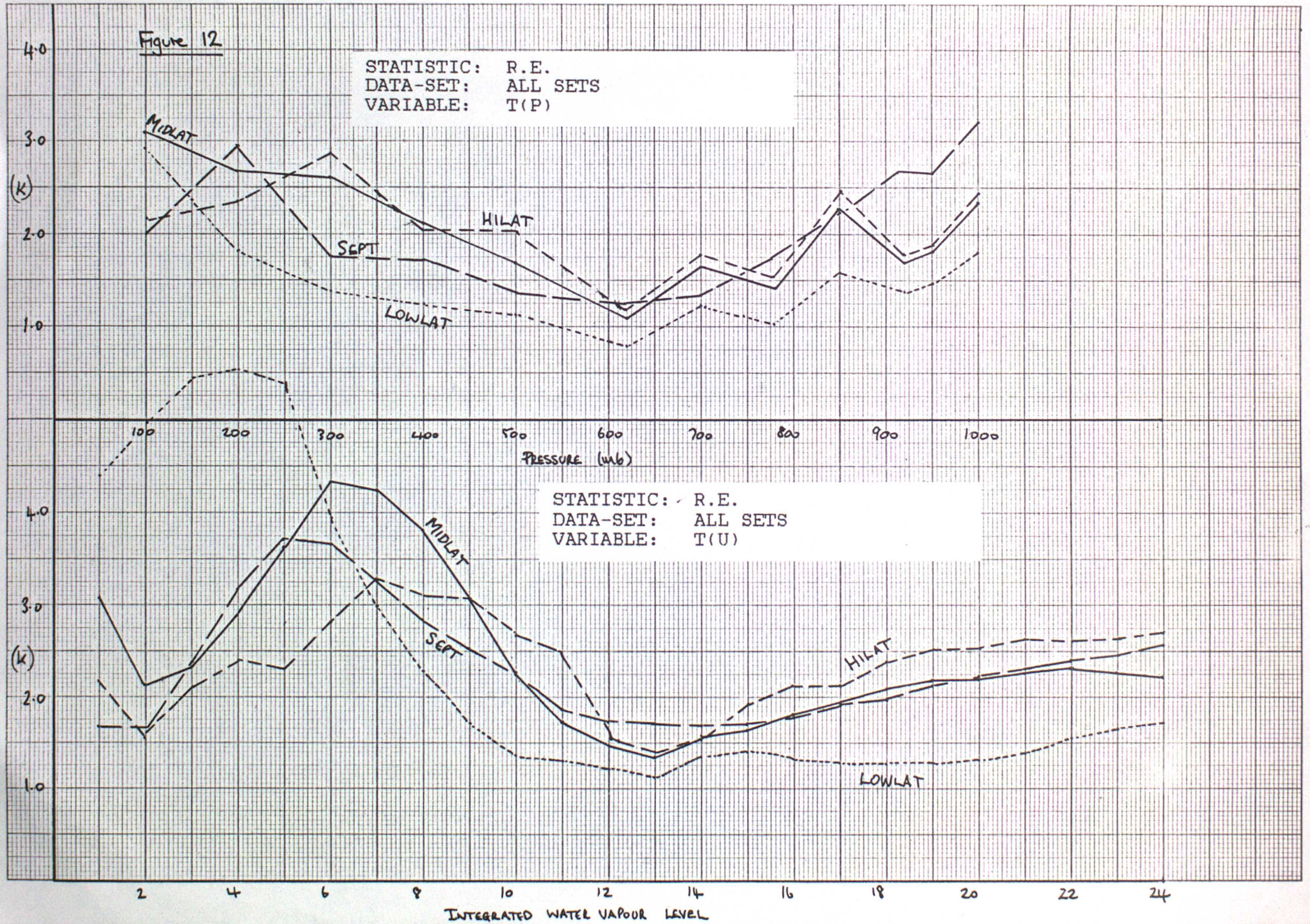
STATISTIC: R.E.
DATA-SET: ALL SETS
VARIABLE: T(P)
MIDLAT
HILAT
SEPT
LOWLAT
4·0
3·0
(K)
2·0
1·0
100
200
300
400
500
600
700
800
900
1000
PRESSURE (mb)
STATISTIC: R.E.
DATA-SET: ALL SETS
VARIABLE: T(U)
MIDLAT
SEPT
HILAT
LOWLAT
4·0
3·0
(K)
2·0
1·0
2
4
6
8
10
12
14
16
18
20
22
24
INTEGRATED WATER VAPOUR LEVEL

Figure 13

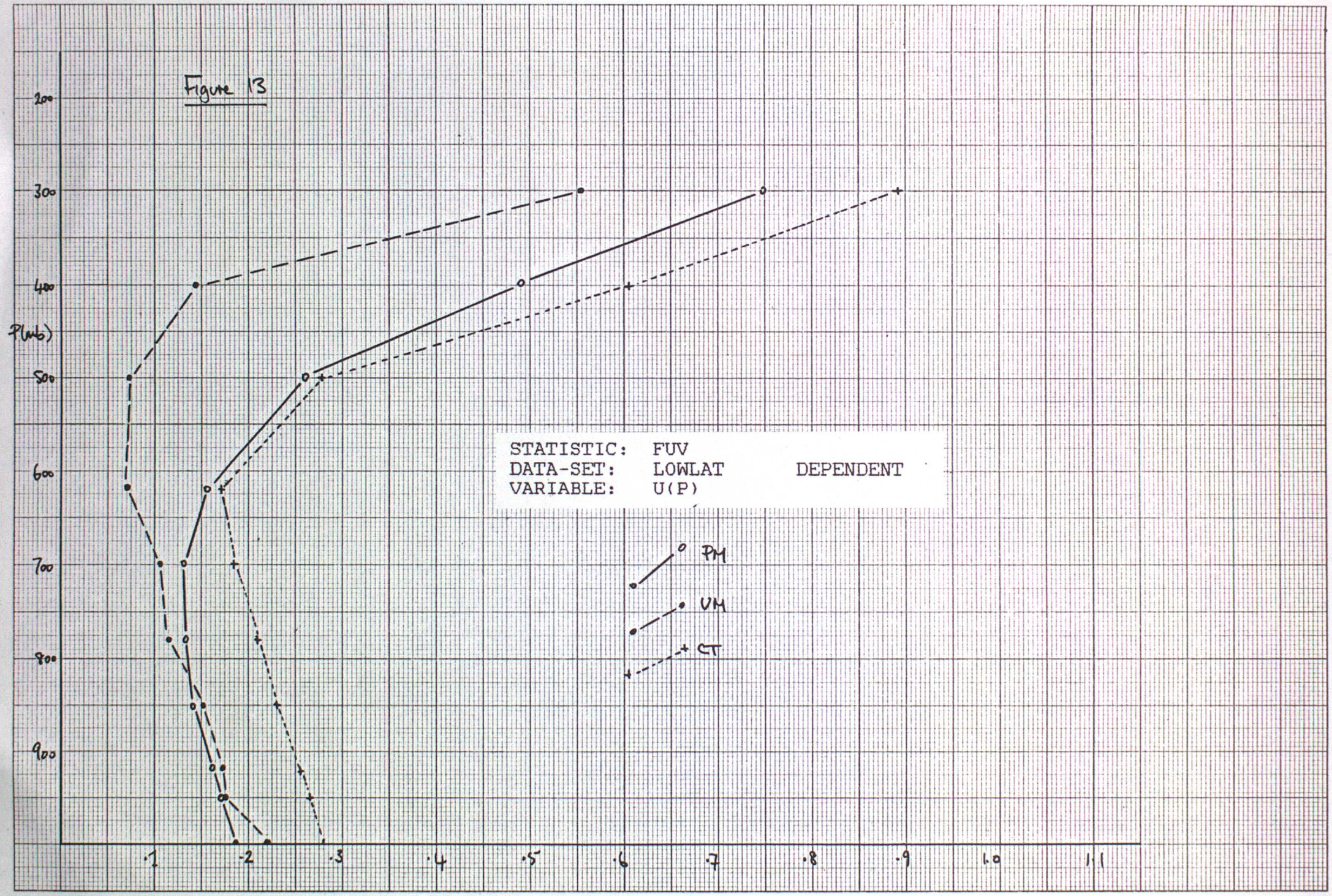
200
300
400
P(mb)
500
600
700
800
900
.1
.2
.3
.4
.5
.6
.7
.8
.9
1.0
1.1
STATISTIC: FUV
DATA-SET: LOWLAT DEPENDENT
VARIABLE: U(P)
PM
VM
CT

Figure 15

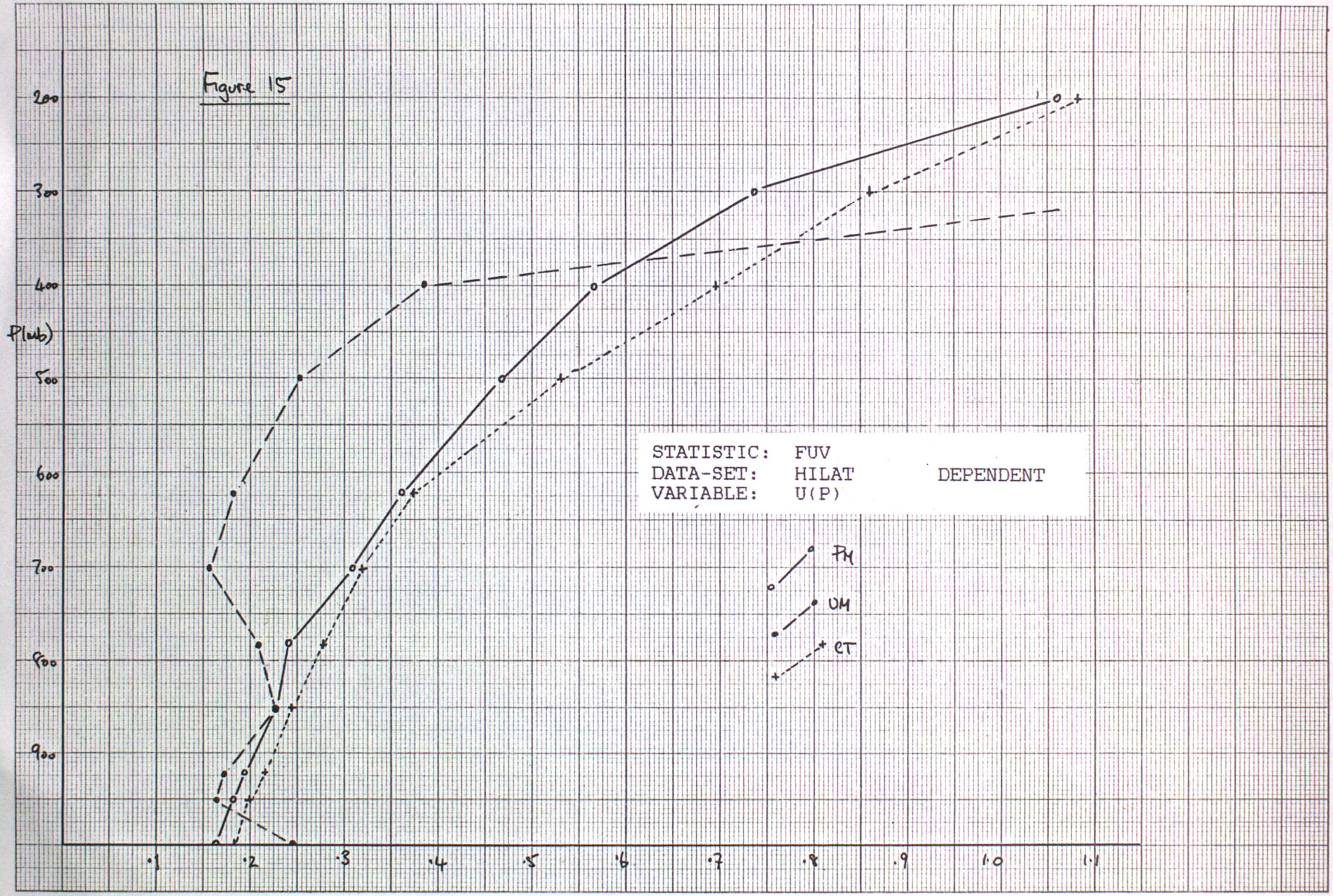
200
300
400
P(mb)
500
600
700
800
900
.1
.2
.3
.4
.5
.6
.7
.8
.9
1.0
1.1
STATISTIC: FUV
DATA-SET: HILAT DEPENDENT
VARIABLE: U(P)
PM
UM
CT

Figure 16

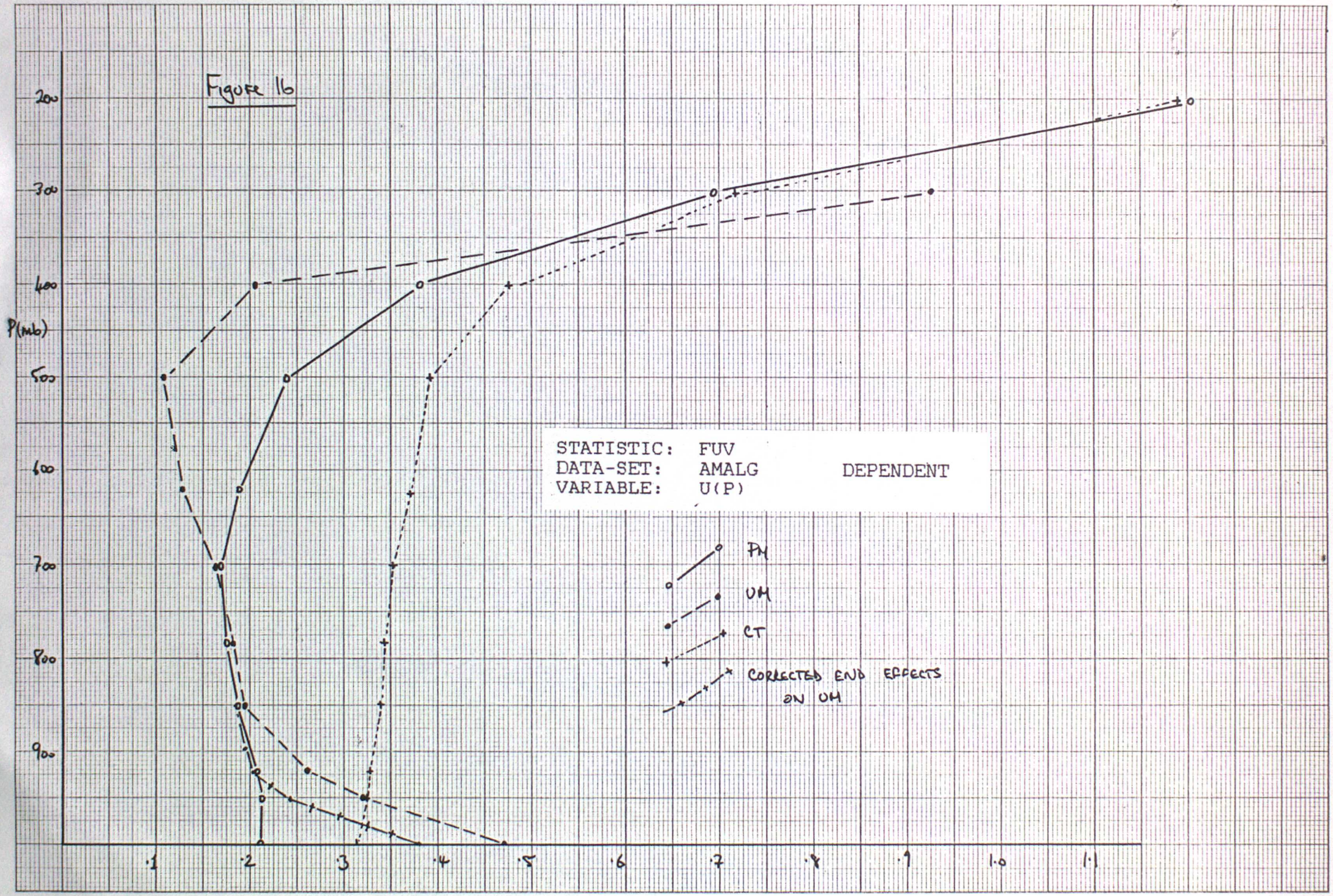
200
300
400
P(mb)
500
600
700
800
900
.1
.2
.3
.4
.5
.6
.7
.8
.9
1.0
1.1
STATISTIC: FUV
DATA-SET: AMALG DEPENDENT
VARIABLE: U(P)
PM
UM
CT
CORRECTED END EFFECTS ON UM

Figure 17

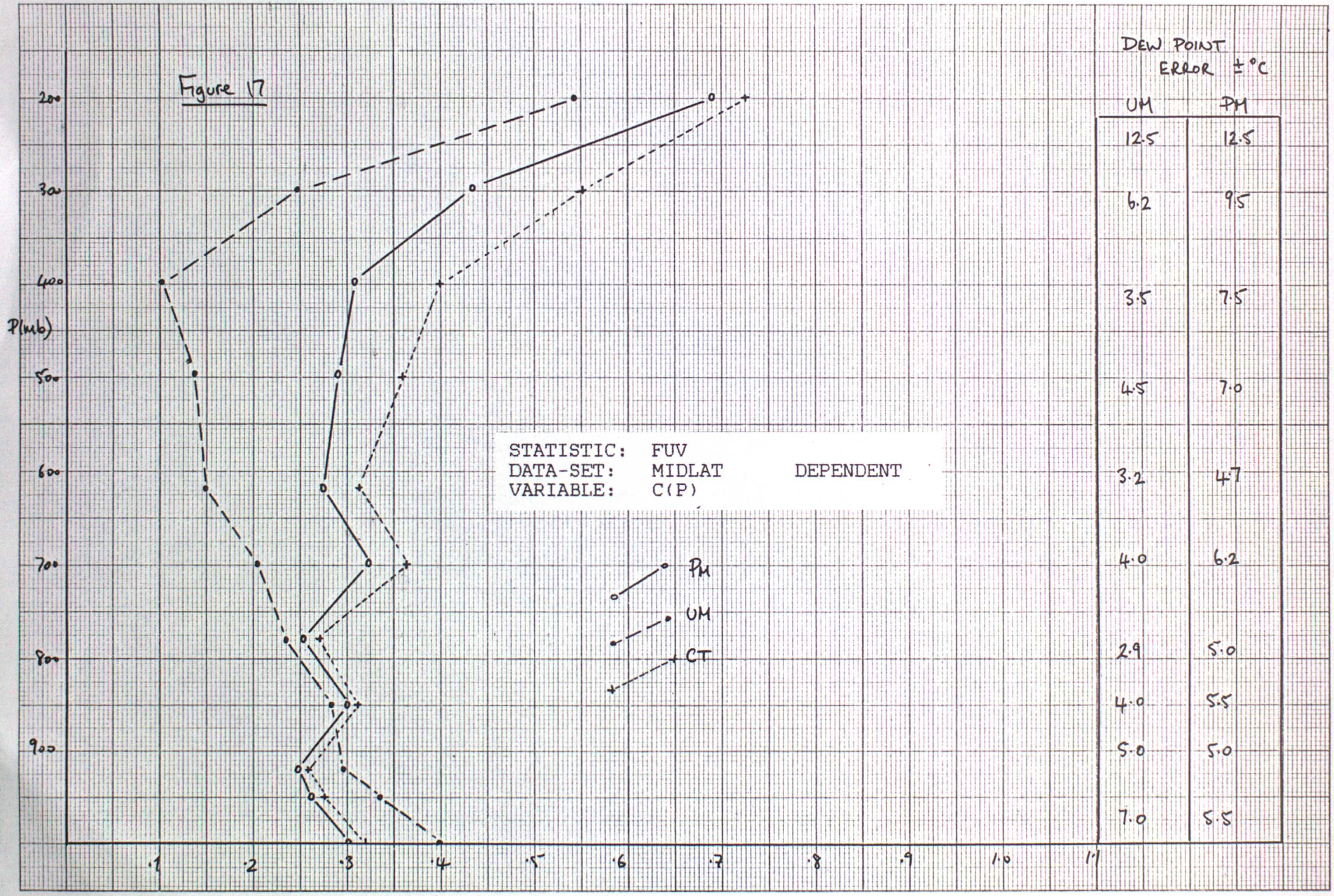

DEW POINT ERROR ±°C

UM	PM
12·5	12·5
6·2	9·5
3·5	7·5
4·5	7·0
3·2	4·7
4·0	6·2
2·9	5·0
4·0	5·5
5·0	5·0
7·0	5·5

Figure 18

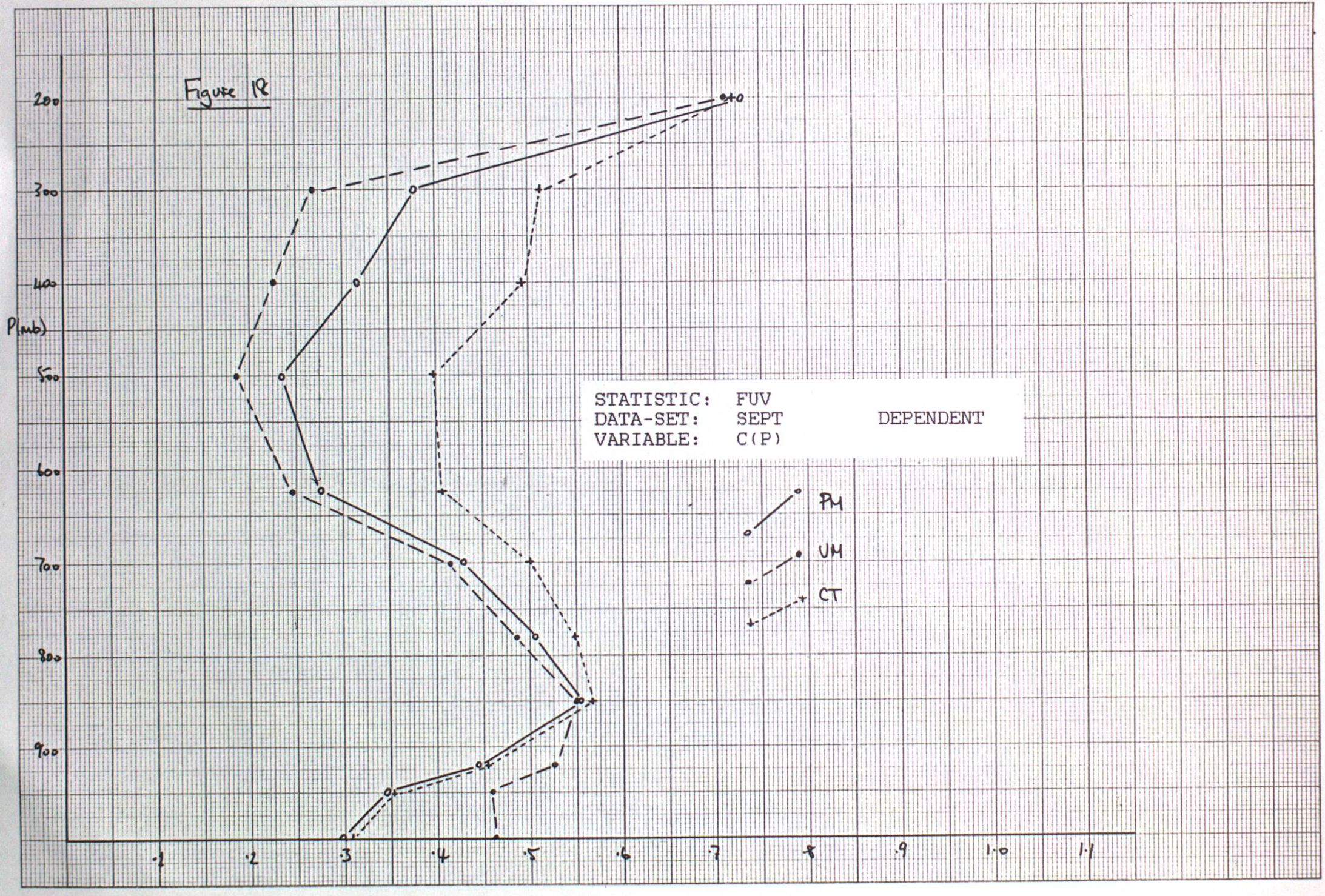
200
300
400
P(mb)
500
600
700
800
900
.1
.2
.3
.4
.5
.6
.7
.8
.9
1.0
1.1
STATISTIC: FUV
DATA-SET: SEPT DEPENDENT
VARIABLE: C(P)
PM
UM
CT

Figure 19 Low Noise

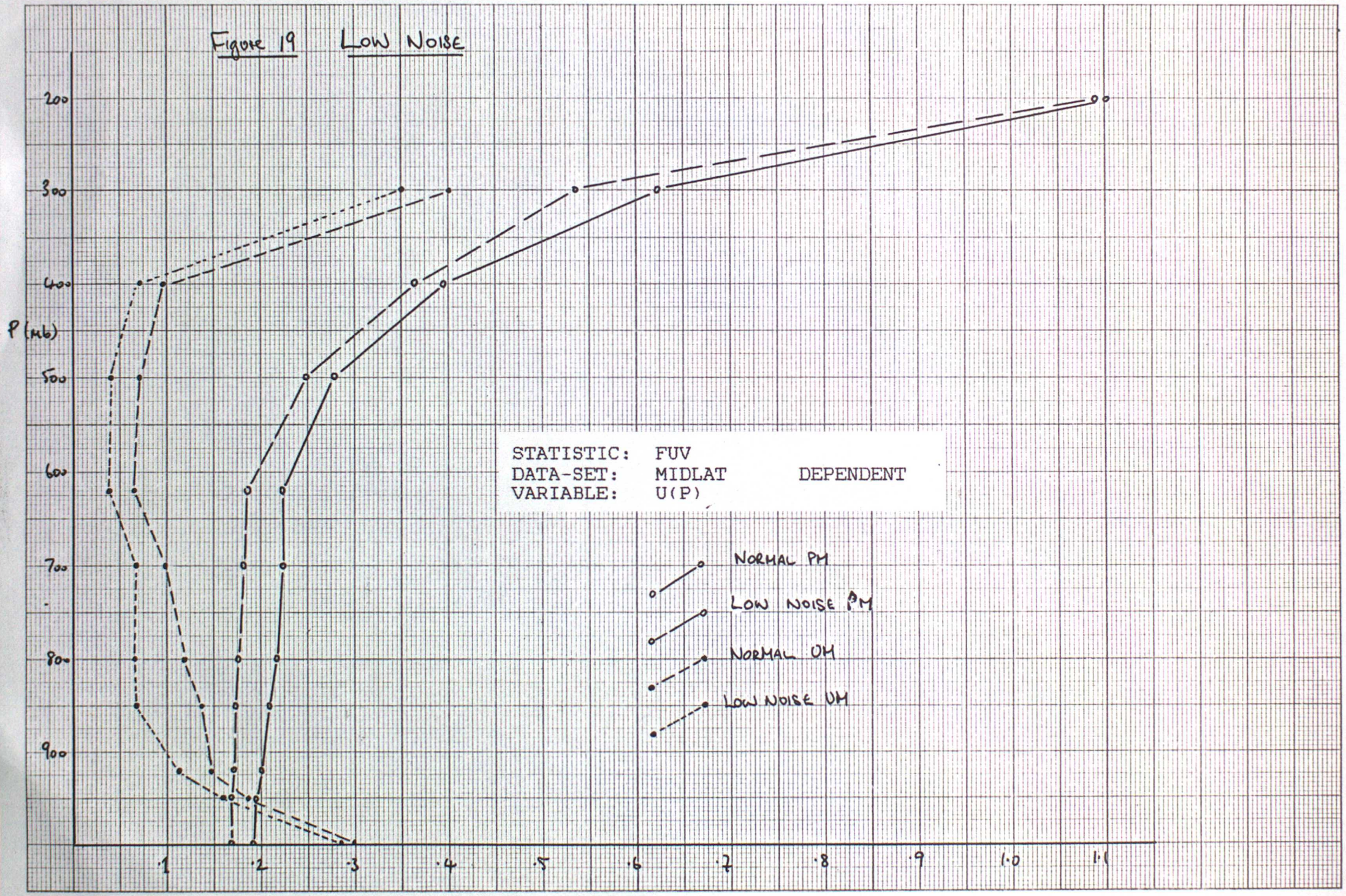

Figure 20 Low Noise

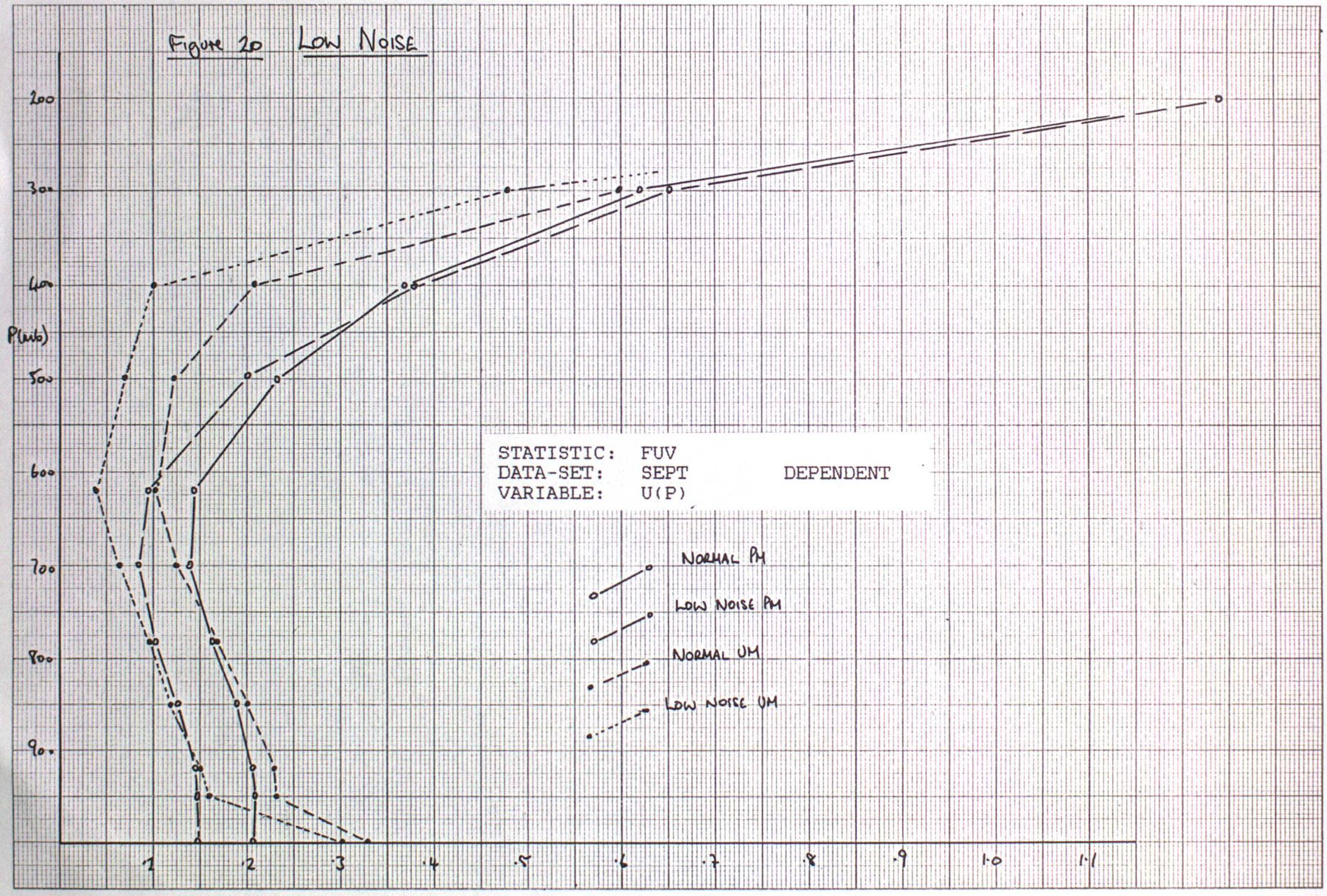

Figure 21 Mismatched Noise

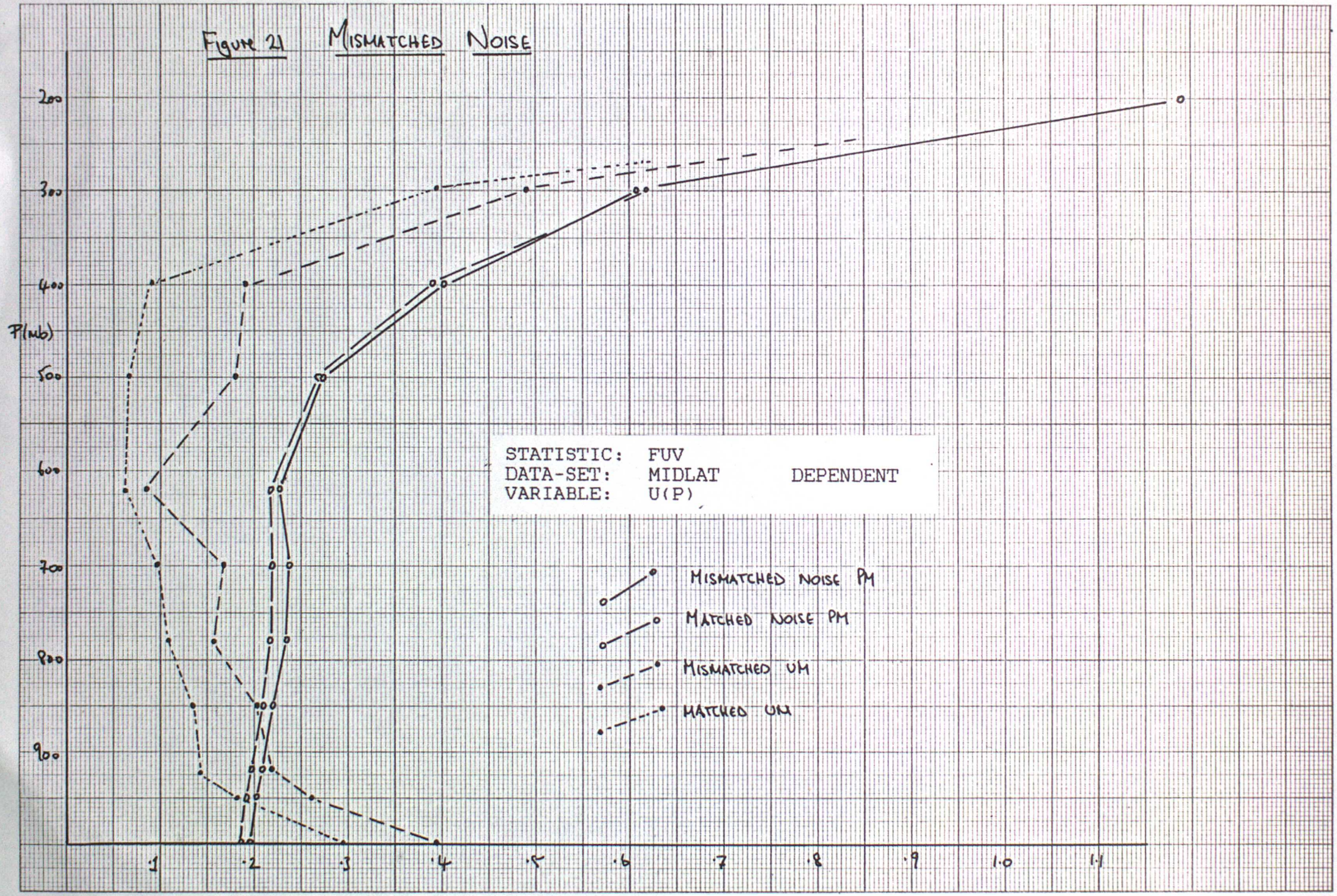

Figure 22 Mismatched Noise